

The Cosmic Evolutionary Theory

Ding-Yu Chung*

The cosmic evolutionary theory describes in details the evolution from the pre-universe to the present universe, including galaxies and elementary particles. In the cosmic evolutionary theory, the evolution of the expanding universe involves four stages: the pre-universe, the pre-expanding universe, the mixed pre-expanding universe, and the expanding universe. No cosmic singularity occurs. In the expanding universe, the two parallel universes, the hidden universe and the observable universe, are different in physical laws. When they are compatible, dark energy emerges to accelerate cosmic expansion in the observable universe. In the observable universe, baryonic matter with four-dimensional space-time is incompatible with dark matter with higher dimensional space-time. The incompatibility increases with the increasing size of the universe. Such incompatibility brings about the formation of inhomogeneous structure (anisotropies in the CMB) where the baryonic matter domains surrounded by the dark matter halos as oil droplets surrounded by water in emulsion. The whole universe behaves as one unit of emulsion that explains in details the evolution of elliptical, normal spiral, barred spiral, irregular, and dwarf galaxies as well as clusters and superclusters. There is duality between cosmic evolution and physical laws. Derived from the cosmic evolution, baryonic matter has the dimensional orbital that resembles to atomic orbital. The dimensional orbital constitutes the periodic table of elementary particles to account for all gauge bosons, leptons, quarks, and hadrons whose masses can be calculated using only four known constants: the number of the extra spatial dimensions in the eleven dimensional membrane, the mass of electron, the mass of Z^0 , and α_e . The calculated masses are in good agreement with the observed values.

1. *From the pre-universe to the expanding universe*

The cosmic evolutionary theory describes in details the evolution from the pre-universe to the present universe, including galaxies and elementary particles. The cosmic evolutionary theory provides the explanations for physical laws, cosmology, astronomical phenomena, the cyclic universe, and elementary particles, including gauge bosons, leptons, quarks, and hadrons whose calculated masses are in good agreement with the observed values. In the cosmic evolutionary theory, the evolution of the expanding universe involves four stages: the pre-universe, the pre-expanding universe, the mixed pre-expanding universe, and the expanding universe. Each stage has different compositions of objects with definite shapes and vacuums with homogeneous spaces. In terms of physical laws, relativity and quantum mechanics do not exist fully until the expanding universe.

Objects and vacuums evolve in different stages. The evolutionary sequence for the evolution of objects is string, membrane, particle, and then particle-wave. For vacuums, it

is object vacuum, single vacuum, inclusive vacuum, and then exclusive vacuum. Object vacuum takes turn to coexist equally with object at the same location. Single vacuum exists with an object at the same location or different locations in one object to one vacuum relation. Inclusive vacuum exists at the same location with multiple objects. Exclusive vacuum excludes object at the same location.

The universe starts with the pre-universe that is object vacuum-object, the equilibrium state between the vacuum and the pairs of ten-dimensional superstring and anti-superstring. The vacuum energy is equal to the non-zero energy of the superstring. Object vacuum can also undergoes vacuum fluctuation as condensation and diffusion. The pre-universe is the platform for multiverse.

The condensation as the compactification of higher dimensions leads to the formation of a two space-time dimensional string and the empty space as single vacuum, each of which associates with one object. One object per vacuum is the definition of fermion. Before the expanding universe, the universe is pre-relativistic and pre-quantum mechanical with instantaneous non-locality and precision instead of locality and probability [1], so the space-time of the 2D-string can attach to the space-time of the adjacent 10D-superstring instantly and precisely. The attached string provides the eleventh dimension to generate an eleven-dimensional membrane. This evolution from string to membrane is the reverse of M-theory that starts with 11D-membrane.

The attached string can undergo vacuum fluctuation and excitation. In terms of vacuum fluctuation, the non-zero vacuum energy causes the attached string to diffuse into single vacuum to become an infinite dimension. Subsequently, the attachment of the string in membrane provides AdS (anti-de Sitter space) for the diffused string to condense (compactify) again. When this diffusion-condensation overlaps with the diffusion-condensation from another membrane, "pregravity" (the predecessor of gravity) is formed. Pregravity is in inclusive vacuum that allows more than multiple objects per vacuum. Boson is defined as multiple objects per vacuum. This diffusion-condensation reproduces the Planck-infinite dimension in the Randall-Sundrum model [2] for gravity. The resulting structure is 9-brane embedded in the eleven-dimensional bulk with pregravity. Since pregravity is active in an empty space, pregravity is a long-ranged force as Fig. 1 and Fig. 2.

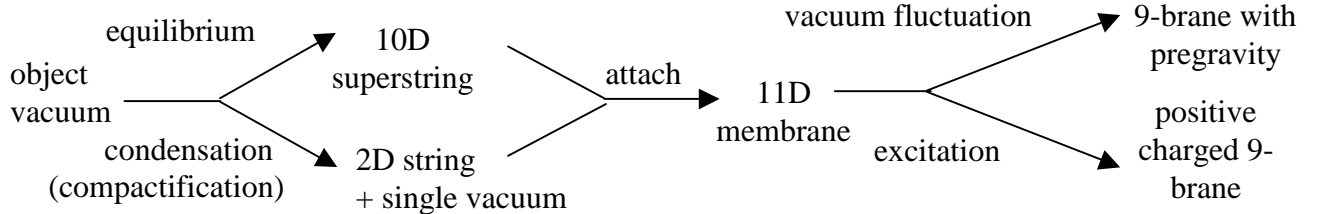


Fig. 1: the evolution of 9-brane in the pre-expanding universe

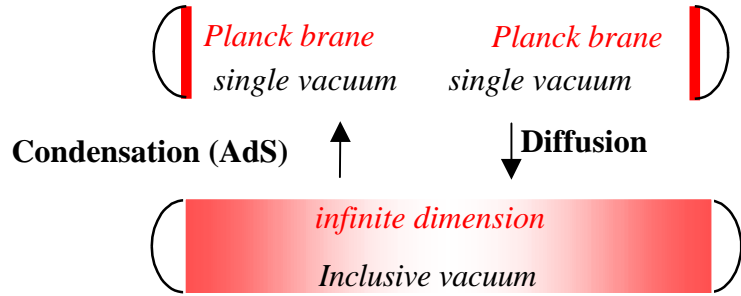


Fig. 2: pregravity as the Randall-Sundrum model

In terms of excitation, the attached string behaves as the 1D circle circling superstring in the 10D x 1D Kaluza-Klein structure. The quantized excitation of the circle brings about the quantized positive pre-charged force (the predecessor of electromagnetism) with the absorption and the emission of the massless particles in exchange with the massless particles from other membranes. Since the pre-charged force is active in empty space, the pre-charged force is a long-ranged force as Fig. 1 and Fig. 3.

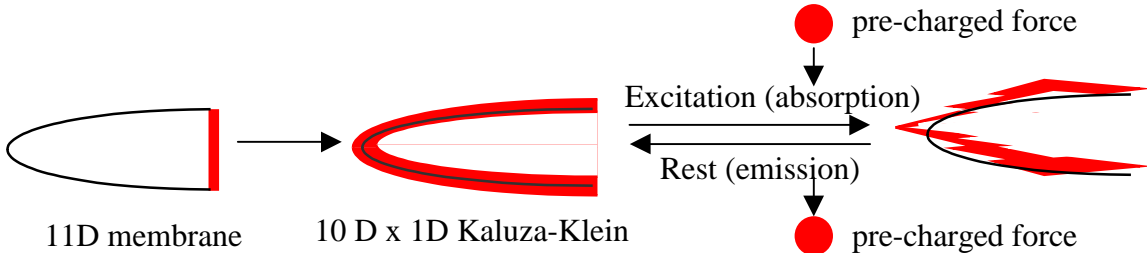


Fig. 3: pre-charged force from excitation

The combination of the vacuum fluctuation and the excitation of the attached string results in the positive charged 9-brane embedded in the eleven-dimensional bulk with pregravity and positive pre-charged force (Fig. 1). At the same time, the ten-dimensional anti-superstring becomes negative charged 9-antibrane embedded in the eleven-dimensional bulk with anti-pregravity and negative pre-charged force.

The original force among strings in the pre-universe is the pre-strong force, the predecessor of the strong force. The force is resulted from the absorption and the emission of massless particles from strings. Since it transmits through object vacuum with non-zero energy, rather than an empty space, it is a short-ranged force through a non-zero energy medium. This pre-strong force remains as a short-ranged force among membranes.

The combination of the 9-brane and the 9-antibrane is the brane-antibrane unit. The structure of the brane-antibrane unit is determined by the evolutionary sequence of the three forces. In the normal evolutionary sequence, the pre-strong force exists first. Then, the emergence of the repulsive force between pregravity and anti-pregravity forces a brane and an antibrane to move away from each other. Subsequently, the pre-strong force

connects the newly formed brane or the antibrane with previously formed branes or antibranes. Finally, the pre-charged force emerges. The space occupied by branes is opposite from the space occupied by antibranes, so branes and antibranes are chiral. This normal evolutionary sequence provides the chiral brane-antibrane unit where the chiral boundary positive charged 9-brane and the chiral boundary negative charged 9-antibrane embedded in the eleven-dimensional space-time are separated by chiral pregravity and chiral anti-pregravity as Fig. 4.

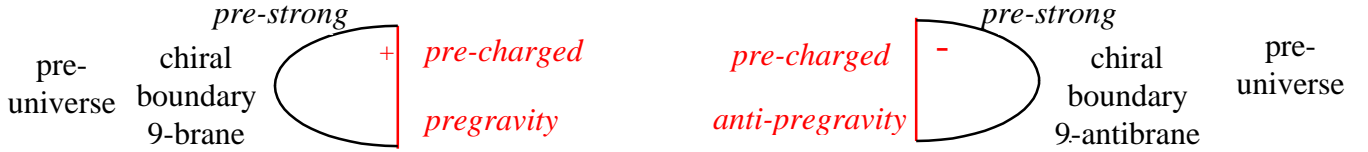


Fig. 4: the pre- expanding universe

The pre-expanding universe emerges with this chiral brane-antibrane unit as the predominant structure. All forces and membranes inside the pre-expanding universes are chiral. The pre-expanding universe continues to grow with the conversion of the pre-universe vacuum entering into the single vacuum in the middle of the pre-expanding universe. This two-brane structure of the pre-expanding universe also appears in the Horava-Witten eleven dimensional pregravity on a manifold with two ten-dimensional boundaries [3], the ekpyrotic universe boundary branes [4], and the brane-antibrane universe [5].

During the steady conversion from the pre-universe to the pre-expanding universe takes place, the total volume of the two universes remain constant. To maintain this constant volume, the attractive force (A) between the positive and negative pre-charged forces is equal to the sum of the repulsive force (R) between pregravity and anti-pregravity, and the special global short-ranged pre-strong force (C) connecting the pre-expanding universe and the pre-universe. $A = R + C$ is a non-localized global relation for the constant total volume of the universes. If $A > R + C$, the total volume is smaller, and if $A < R + C$, the total volume is larger.

There is a small amount of the abnormal evolutionary sequence in the pre-expanding universe. In the abnormal evolutionary sequence, the pre-strong force exists first. Then, the emergence of the attractive force from the pre-charged forces draws the brane and the antibrane together. The combined brane-antibrane units go impartially to either side of the pre-expanding universe, resulting in the achiral brane-antibrane units. (Essentially, attractive force and repulsive force are the tools to form chirality and achirality.) Finally, pregravity and anti-pregravity emerge. In the universe, local interactions are either chirality-specific or achirality-specific. Unable to interact with the region inside the chiral pre-expanding universe, the achiral brane-antibrane units are separated from the chiral pre-expanding universe, and congregate in the area connecting the pre-universe and the pre-expanding universe. The result is the decrease of the connection between the pre-expanding universe and the pre-universe. However, as a non-localized global relation, $A = R + C$ continues with the right amount of C contributed by

the pre-universe as long as there is still connection between the pre-universe and the pre-expanding universe.

As the pre-expanding universe grows with the chiral brane-antibrane units, the number of the achiral brane-antibrane units grows. Eventually, the pre-expanding universe is disconnected completely from the pre-universe by the achiral brane-antibrane units. Without C, the excess attractive force ($A > R$) between positive branes and negative charged antibranes causes the pre-expanding universe to collapse, and the repulsive force between pregravity and anti-pregravity causes the pre-expanding universe to inverse. As the 9-brane and the 9-antibrane move toward each other, the 9-brane and the 9-antibrane turn inside, and pregravity and anti-pregravity turn outside. The "gulf" separating the pre-expanding universe and the pre-universe is formed. Eventually, the 9-brane and the 9-antibrane coalesce. At the end of the coalescence, the repulsion between pregravity and anti-pregravity causes a bounce after the collapse.

At this point, the complete coalescence leads to the complete annihilation of brane and antibrane. (Without exclusive vacuum, the annihilation does not lead to radiation that vacates its position continuously.) The annihilation brings about the losses of the membrane property, the pre-charged force, the pre-strong force, and chirality. The result is the generation of the achiral mixed 9-particle with the multiple dimensional Kaluza-Klein structure without the requirements for identical space dimensions and a fixed number of space dimensions as in superstring. All forces formed previously become achiral. The bounce results in the mixed pre-expanding universe, consisting of four equal parts: two groups of achiral mixed 9-particles, achiral pregravity, and achiral anti-pregravity as Fig. 5.

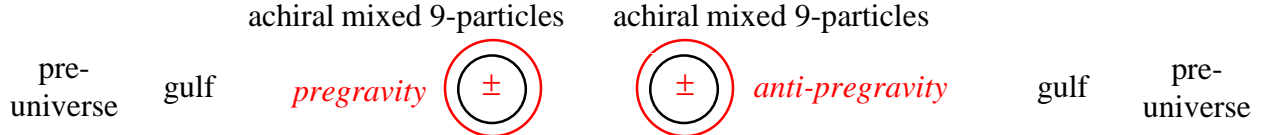


Fig. 5: the mixed pre-expanding universe

The interactions between branes in the form of collision are proposed in various brane models [4, 5, 6]. The cyclic universe model based on the ekpyrotic universe [7] has the collapse-singularity-bounce scheme.

The size of the pre-expanding universe is determined by the ratio between the number of the chiral units and the number of the achiral units. The pre-universe and the mixed pre-expanding universe are different in the composition of objects and vacuums, and are separated from each other permanently. Consequently, the two universes are completely transparent to each other. Without relation with the pre-universe, the mixed pre-expanding universe has zero vacuum energy instead of the non-zero vacuum energy as the pre-universe. With zero vacuum energy and the Kaluza-Klein structure without a fixed number of space dimensions, the mixed 9-particles have potential to fractionalize into multiple lower energy and lower dimensional mixed particles precisely and instantly in the pre-quantum mechanical and pre-relativistic universe. The fractionalization leads to the cosmic expansion into the completely transparent pre-universe. It is the start of the expanding universe. To the pre-universe, the expanding universe is a missing region.

The cosmic expansion mechanism is discussed in Section 2. The two different modes of the cosmic expansion are described in Section 3. The formation of inhomogenous structure in the observable universe is described in Section 4. The evolution of galaxies is stated in Section 5. In Section 6, the cyclic universe is proposed. The derivation of quantum mechanics is described in Section 7. In Sections 8, 9 and 10, the periodic table of elementary particles is constructed to account of all leptons, quarks, gauge bosons, and hadrons, and their masses are calculated.

2. *The cosmic expansion mechanism: the uneven supersymmetry*

In the normal supersymmetry, the repeated application of the fermion-boson transformation transforms a fermion from one point to the same fermion at another point with the same vacuum energy. Such supersymmetry transformation at the same vacuum energy is the normal “even” supersymmetry. At the gradually decreasing vacuum energy as in the cosmic expansion, the supersymmetry is “uneven”. At the gradually decreasing vacuum energy, the uneven supersymmetry transforms the mixed 9-particle fermion (with the Kaluza-Klein structure) from one point to the mixed 8-particle fermion with a lower mass at another point. (In the Kaluza-Klein structure, the space dimensions do not have to be the same, and the number of space dimensions is not fixed.) Therefore, the stepwise repeated uneven supersymmetry transformations expand the universe, and fractionalize the mixed 9-particle into lower dimensional mixed particles from 8 to 3 with decreasingly lower masses.

These stepwise transformations constitute the dimensional hierarchy [8,9] where masses decrease with the space-time dimension numbers. The uneven supersymmetry transformation from D (dimensional number) fermion to D-1 boson at the decreasing vacuum energy is expressed as

$$M_{D-1, B} = M_{D, F} \alpha_{D, F}, \quad (1)$$

where $M_{D-1, B}$ and $M_{D, F}$ are the masses for B_{D-1} and F_D , respectively, and $\alpha_{D, F}$ is the transformation constant, which is same as the fine structure constant, the probability of a fermion emitting or absorbing a boson. The uneven supersymmetry transformation from boson B_D into fermion F_D at decreasing vacuum energy is expressed as

$$M_{D, F} = M_{D, B} \alpha_{D, B} \quad (2)$$

With such repeated uneven supersymmetry transformations at decreasing vacuum energy, various dimensional particles are generated. Assuming α is the same for all fermions and bosons, Eq. (3) for the energy relation among the dimensional bosons is derived.

$$M_D = M_P \alpha^{2(11 - D)} \quad (3)$$

where M_P is the Planck mass, the mass of the eleventh dimensional boson, D = from 4 to 11, and α is the transformation constant and fine structure constant. As shown later in Table 1, all α 's except one is equal to the fine structure constant for electromagnetic field, so Eq. 3 is approximately correct.

3. The expanding universe: the big band and the big bang

The cosmic expansion in terms of the uneven supersymmetry transformation has two different modes for the two sides of the expanding universe: the big band mode for the hidden universe and the big bang mode for the observable universe as Fig. 6.

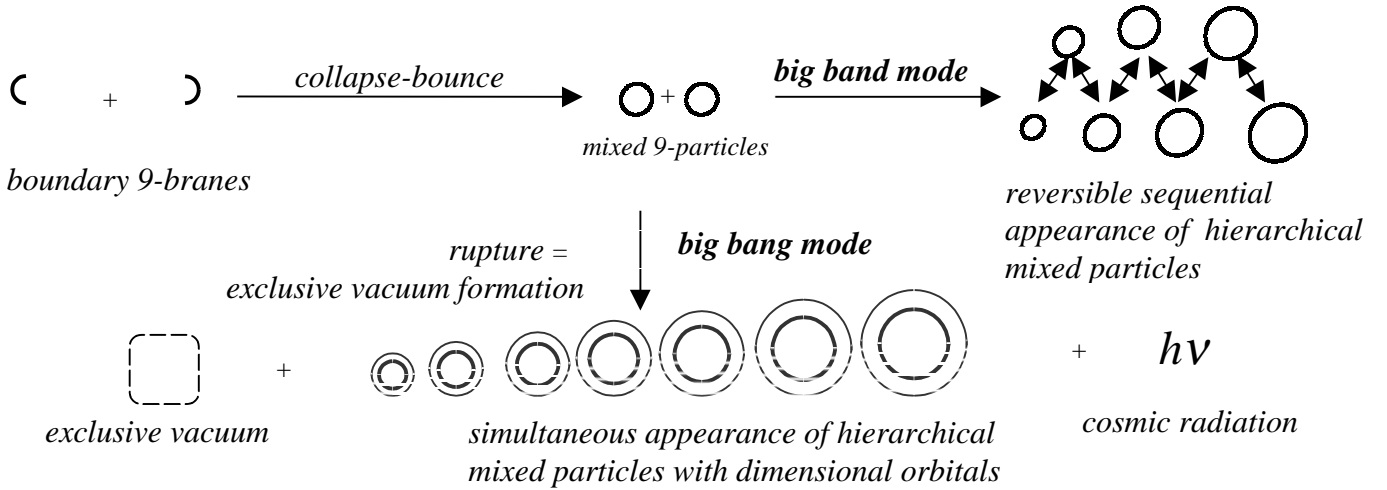


Fig. 6: the big band mode and the big bang mode

The big band mode is used in the hidden universe. In the big band mode, the mixed 9-particle is fractionalized into the hierarchical mixed particles from 3 to 9, whose masses follow the hierarchical dimensional mass formula as Eq. (3) where p particle has $p + 1$ space-time dimension, D . In the big band mode, through slow decrease in vacuum energy, the slow sequential stepwise fractionalization from the mixed 9-particle to the mixed 3-particle results in the slow cosmic expansion. Without entropy, it is reversible, so at the end of the cosmic expansion, the hidden universe undergoes slow condensation back to the mixed 9-particle. The hidden universe undergoes expansion and contraction, like a big elastic rubber band (big band) as the top figure in Fig. 6.

The big bang mode is used in the observable universe. In the big bang mode, the fractionalization is extremely rapid by rapid decrease in vacuum energy, resulting in the superluminal inflation that ruptures the observable universe. (The ease of rupture is proportional to the rate of expansion.) Consequently, all mixed particles are not held together, and are separated by exclusive vacuum as the gap among particles. Exclusive vacuum excludes objects. At the end of the superluminal inflation period, a mixture of mixed particles from 9 to 3 with exclusive vacuum emerges.

The mechanism to generate exclusive vacuum is to assign positive and negative charges to the two internal boundary branes within the mixed particle, resulting in the dislocation of energy by the internal annihilation (implosion). The dislocation of energy from the mixed particle results in exclusive vacuum as the empty mixed 3-particle and massless cosmic radiation as the dislocated energy. Exclusive vacuum is the space left behind by moving cosmic radiation.

The mixed particles that are not annihilated have asymmetrical charge-parity (CP asymmetry), in such way that the mixed particle has two asymmetrical sets (main and auxiliary) of space dimensions from the two boundary branes within the mixed particle. The auxiliary set is dependent on the main set, so the mixed particle appears to have only one set of space dimensions. Such two asymmetrical sets of space dimensions form the base for the periodic table of elementary particles [8]. The degree of the rupture is determined by the ratio between the CP symmetry and the CP asymmetry. (The CP asymmetry to generate matter is the predecessor of the CP nonconservation.)

After the rupture, particles become isolated by the gap (exclusive vacuum) among them. Such gap disrupts non-locality, resulting in locality for each particle [1]. Such independent locality leads to randomness instead of precise coordination. Quantum mechanics (probability), relativity (locality), and entropy emerge. The summary of the cosmic evolution is described in Fig. 7.

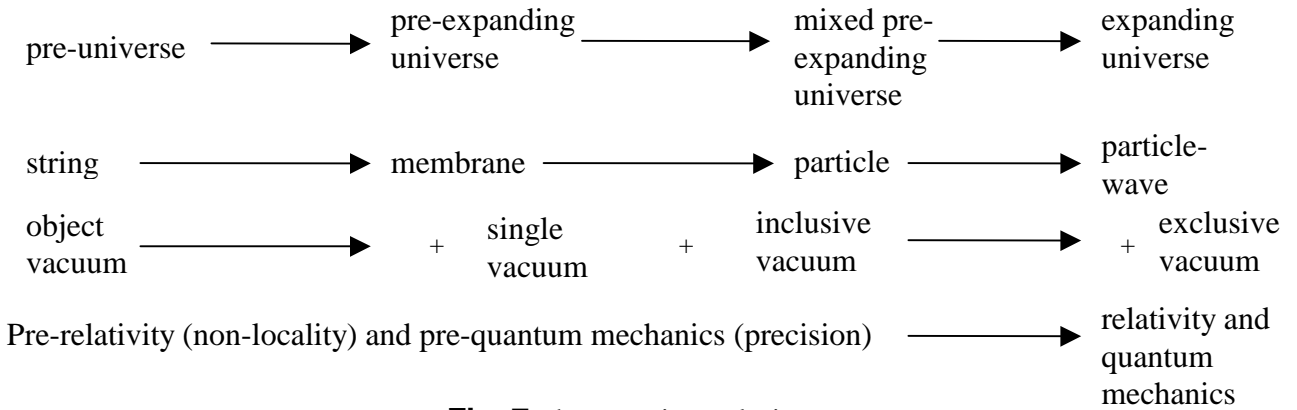


Fig. 7: the cosmic evolution

Without precision and non-locality, the fractionalization in the observable universe stops after the rupture. The two fractionalizations in the opposite sides (hidden and observable) of the expanding universe are chiral. This chiral fractionalization is the predecessor of the chiral weak interaction.

Exclusive vacuum and cosmic radiation emerge only after the superluminal inflationary emergence of all of the hierarchical mixed particles. Consequently, the superluminal inflationary emergence of the mixed particles followed by the non-inflationary emergence of cosmic radiation constitutes the hybrid inflation [9]. Cosmic radiation, observable elementary particles, all force fields, relativity, and quantum mechanics emerge only at the end of inflation.

The hidden universe and the observable universe are incompatible in dimensionality and in physical laws (with and without exclusive vacuum, relativity and quantum mechanics), so they are completely transparent to each other until they are compatible in dimensionality. This two-universe model appears also in the two-universe (visible and hidden) model in the cyclic ekpyrotic universe model [7].

4. *The formation of inhomogeneous structure in the observable universe*

The observable universe consists of the mixed particles from 3 to 9 (from 4D to 10D) in the forms of baryonic matter and dark matter. The baryonic matter consists of the mixed 3-particle (4D). Dark matter consists of the mixed particles from 4 to 9 (from 5D to 10D). Both dark matter and baryonic matter share the same long-ranged gravity. As shown later, dark matter does not have electromagnetism, so it cannot be seen, but it can be observed by gravity. Dark matter exists in the form of neutral gas. There are seven mixed particles from 9- to 3-particle. Baryonic matter is one of the seven mixed particles at equal mass proportions, so the baryonic mass fraction is 1/7 (0.14). The universal baryonic mass fraction was found to be 0.13 by the observations of primordial deuterium abundance [10]. The calculated value agrees well with the observed value.

The extra space dimensions in dark matter protrude outside of 4D space-time, so dark matter and baryonic matter are dimensionally incompatible to each other, like oil and water in emulsion. Cosmic radiation (any massless particles) is compatible with both baryonic matter and dark matter. The incompatibility between baryonic matter and dark matter increases linearly with decreasing temperature of cosmic radiation whose temperature decreases with increasing size of the universe. Thus, the incompatibility increases with increasing size of the universe. The whole universe behaves as one unit of emulsion. The mass ratio between baryonic matter and dark matter is 1 to 7. As water domains surround oil droplets (the smaller part) in emulsion, dark matter domains surrounded baryonic droplets (the smaller part). These dark matter domains later became the spherical dark matter halos surrounding galaxies. The baryonic droplets became galaxies.

In the cosmic evolutionary theory, quantum mechanics is fully developed only at the end of the inflation. The inflation is a non-local phenomenon without local quantum fluctuation. Local quantum fluctuation simply does not exist during the inflation. In the standard inflation theory [11], quantum fluctuations during the inflation are stretched exponentially so that they produce anisotropies in the CMB (cosmic microwave background). However, without fine-tuning, the calculated amplitude of the density perturbation induced by quantum fluctuations during the inflation is much larger than the observed amplitude in CMB. It is a serious problem in the inflation theory [12]. In the cosmic evolutionary theory, the dimensional incompatibility between dark matter and baryonic matter produces anisotropies in the CMB.

As in emulsion, the size of the baryonic droplet increases with increasing incompatibility between dark matter and baryonic matter. Baryonic matter can exist as free baryonic matter among dark matter or as baryonic matter in the baryonic droplet. At the

beginning of the expanding universe with high cosmic radiation temperature, baryonic matter and dark matter were completely compatible with each other, and baryonic matter existed entirely as free baryonic matter. As the size of the universe increased, the size of the baryonic droplets increased with the increasing incompatibility between baryonic matter and dark matter. At the time of recombination (neutralization), the baryonic matter in the small baryonic droplets coexisted with free baryonic matter in the surrounding. With electromagnetic attraction, the baryonic droplet had higher matter density than the surrounding dark matter without electromagnetism and isolated free baryonic matter. The density difference between the baryon matter in the baryonic droplet and the baryonic matter in the surrounding leaded to anisotropies observed in the CMB.

When the CMB occurred moment before the recombination, because of radiation pressure, the density in the baryonic droplet was much lower than the normal density without radiation pressure. After the decoupling between baryonic matter and radiation at the recombination, the absence of radiation pressure allowed the density of the droplet to return to the normal density quickly.

As the universe expanded, the increasing incompatibility drove increasing amount of free baryonic matter into the baryonic droplets. The growth of the baryonic droplet by the increasing incompatibility from the cosmic expansion coincided with the growth of the baryonic droplet by gravity from the cosmic expansion. The pre-galactic universe consists of the growing baryonic droplets surrounded by the dark matter halos, which connected among one another in the form of filaments and voids.

The dimensional incompatibility between the baryonic droplet and the dark matter halo is expressed as the interfacial zone between the two different matter domains. The interfacial zone involves an additional dimension between four-dimensional baryonic matter and higher dimensional dark matter as in the two-sided Randall - Sundrum model [2] as Fig. 8.

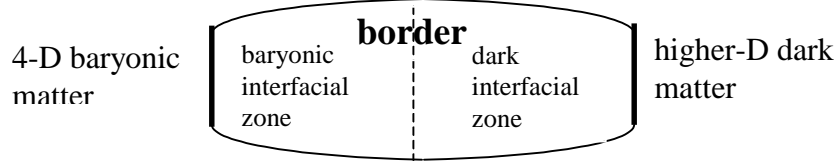


Fig. 8: the anti-expansion force in the interfacial zone in the two-sided Randall – Sundrum model between baryonic matter and dark matter

The baryon-dark border between baryonic matter and dark matter is in the middle of the interfacial zone. The interfacial zone consists of the dark interfacial zone and the baryonic matter zone for two sides of the baryon-dark border. The force in the interfacial zone is the anti-expansion force as the enhancement of gravity in the interfacial zone away from the baryon-dark border to maintain a clear border. Such enhancement of gravity is same as the enhancement of gravity in the M. Milgrom's [13] Modified Newtonian Dynamics (MOND). In the equilibrium state, the enhanced gravity in the interfacial zone is constant for both baryonic interfacial zone and dark interfacial zone, resulting in the zero net anti-expansion force and the unchanged border. Such constant enhanced gravity in the baryonic interfacial zone results in flat rotation curves as observed in some galaxies [14].

In MOND, the acceleration at the starting line of the anti-expansion zone is a_0 . The interfacial zone with the enhanced gravity has acceleration less than a_0 , while the area with the acceleration greater than a_0 has normal gravity. The distance from the center of baryonic mass to the starting line of the interfacial zone increases with decreasing a_0 and increasing total mass from the center to the starting line. At the baryon-dark border, the acceleration is a_b . The distance from the center to the baryon-dark border increases with decreasing a_b and increasing total mass from the center of baryonic mass to the baryon-dark border. The size of the universe is directly proportional to a_0 and a_b .

As the incompatibility between dark mater and baryonic matter increases with increasing size of the universe, the droplet develops the droplet growth potential as the potential to increase the mass of the droplet. The droplet growth potential converts to the non-zero net anti-expansion force by moving the baryon-dark border outward to absorb free baryonic matter outside and to merge with other droplets. Such movement of the baryon-dark border is derived from the uneven enhancement of gravity in the interfacial zone: high enhancement of gravity in the dark interfacial zone and low or no enhancement of gravity in the baryonic interfacial zone. This low or no enhancement of gravity in the baryonic interfacial zone is observed as falling rotation curves in bright galaxies [14].

In the case of the trapping of free dark matter inside the baryonic droplet, the incompatibility between dark matter and baryonic matter generates the droplet contraction potential. The potential is to contract the droplet in order to remove the free dark matter inside. The droplet contraction potential converts to the non-zero net anti-expansion force by moving the baryon-dark border inward to expel free dark matter inside. The inward movement involves the uneven enhancement of gravity: low enhancement in the dark interfacial zone and high enhancement of gravity in the baryonic interfacial zone. The high enhancement of gravity in the baryonic interfacial zone is observed as rising rotation curves in dwarfs and low surface brightness galaxies [14].

5. *The evolution of galaxies, clusters, and superclusters*

When there were many baryonic droplets, the merger among the baryonic droplets became another mechanism to increase the droplet size and mass. In Fig. 9, the baryonic droplets (A and B) merged into one droplet (C). When three or more droplets merged together, dark matter was likely trapped in the merged droplet (D, E, and F in Fig. 9). The droplet with trapped dark matter inside is the heterogeneous baryonic droplet, while the droplet without trapped dark matter inside is the homogeneous baryonic droplet.

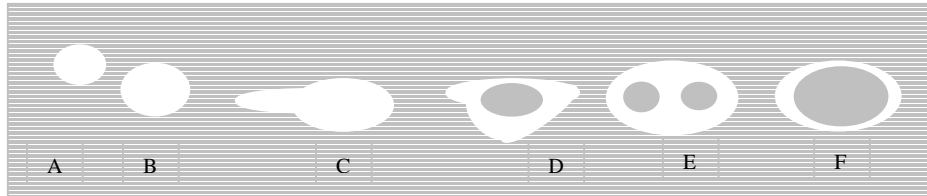


Fig. 9: the homogeneous baryonic droplets (A, B, and C), and the heterogeneous baryonic droplets (D, E, and F)

For the heterogeneous droplet, the dark matter core is essentially the dark droplet surrounded by the baryonic matter shell. As the baryonic droplet, the dark matter core has the droplet growth potential proportional to the size of the universe. As the baryonic droplet, the dark matter core with the growth potential has the baryon-dark border moving toward the baryonic matter shell. Thus, two baryon-dark borders are the external border between the dark matter halo and the and the dark matter halo and the internal baryon-dark border between the baryonic matter shell and the dark matter core. The external border moved toward the dark matter halo, while the internal border moved toward the baryonic matter shell. When a section of the internal border and a section of the external border merged, the dark matter from the dark matter core moved to the dark matter halo away from the heterogeneous droplet, and the droplet became homogeneous.

When the temperature dropped to $\sim 1000^{\circ}\text{K}$, some hydrogen atoms in the droplet paired up to create molecular baryonic matter. The most likely place to form such molecular baryonic matter was in the interior part of the droplet. For heterogeneous droplet, molecular baryonic matter formed a molecular layer around the core. Molecular hydrogen cooled the molecular layer by emitting infrared radiation after collision with atomic hydrogen. Eventually, the temperature of the molecular layer dropped to around 200 to 300°K , reducing the gas pressure and allowing the molecular layer to continue contracting into gravitationally bound dense layer with high viscosity.

Without electromagnetism, the viscosity of dark matter remained low. The viscosity in the dense molecular layer around the core slowed the movement of the internal baryon-dark border toward the baryonic matter shell. On the other hand, the low-viscosity dark matter did not hinder the movement of the external baryon-dark border toward the dark matter halo. The increasing difference in the speeds of movement between the internal and external borders increased the fraction of the heterogeneous baryonic droplets.

Subsequently, the whole baryonic matter shell became the dense molecular layer. The dense molecular layer contracted into gravitationally bound clumps, which prevented the movement of the internal border. The dark matter cores build up the internal pressure from the accumulated droplet growth potential. Eventually, the core with high internal pressure caused the eruption to the droplet. The dark matter rushed out of the droplet within a short time, and the baryonic matter shell collapsed. This eruption is much larger in area and much weaker in intensity than supernova. The “big eruption” of the baryonic droplet brings about the morphologies of galaxies.

The morphologies of galaxies are dependent on the relative sizes of the dark matter core to the baryonic matter shell and the condition of the opening on the baryonic matter shell. If there was very small or no dark matter core as in the homogeneous baryonic droplet, the shape of the resulting galaxy is circular as in the E_0 type elliptical galaxy. If the relative size of the dark matter core was small, the change in the shape of the shell was minor. It is like squeezing out orange juice (dark matter core) through one opening on the orange skin (baryonic matter shell). As the dark matter core moved out, the baryonic matter shell stretched in the opposite direction. The minor change resulted in an elliptical shape as in E_1 to E_7 elliptical galaxies, whose lengths of major axes are proportional to the relative sizes of the dark matter core.

During the collapse of the baryonic matter shell, the collision produced a shock front of high density, which resulted in the formation of the massive first stars. After few million years, such massive first stars became supernovas and black holes. The supernova shock wave induced the formation of stars in the exterior part of the droplet. The time difference in the formations of the nucleus and the formation of stars in the surface was not large, so there are small numbers of observed young stars in elliptical galaxies.

The early galaxies are quasar galaxies with black holes at the centers of galaxies. The first quasar galaxies that assembled as early as in $2 - 3 \times 10^8$ years after the Big Bang have about the same sizes as the Milky Way [15]. The sizes of early galaxies were large during the early universe, in agreement with the early formation of large galaxies proposed here, and not in agreement with the conventional hierarchical formation of large galaxies from the mergers of small galaxies.

If the size of the dark matter core is medium (D in Fig. 9), it involves a large change on the baryonic matter shell. It is like to release air (the dark matter core) from a balloon (the baryonic matter shell) filled with air. As the dark matter core moved out, the baryonic matter shell moved in the opposite direction.

If there was only one opening as an air balloon with one opening, the dark matter stream from the dark matter core and the baryonic stream from the baryonic matter shell moved in opposite directions. Later, the two streams separated. The dark matter stream merges with the surrounding dark matter. The baryonic stream with high momentum penetrated the surrounding dark matter halo. As the baryonic stream penetrated into the dark matter halo, it met resistance from the anti-expansion force. Eventually, the stream stopped.

The minimization of the interfacial area due to the incomparability between baryonic matter and dark matter transformed the shape of the stream from linear to disk. (The minimization of the interfacial area is shown in the water bead formation on a wax paper.) To transform into disk shape, the stream underwent differential rotation with the increasing angular speeds toward the center. The fast angular speed around the center allowed the winding of the stream around the center. After few rotations, the structure consisted of a bungle was formed by wrapping the stream at the center and the attached spiral arms as spiral galaxy as Fig. 10.

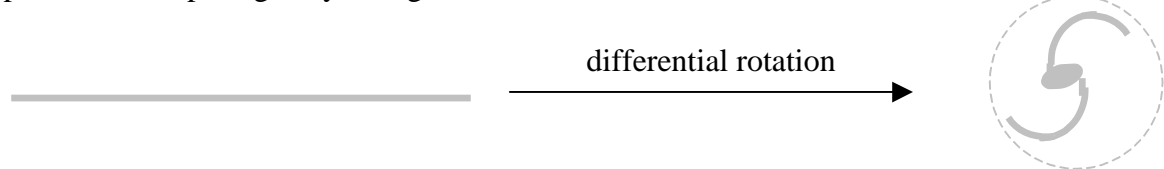


Fig. 10: from the linear baryonic stream to normal spiral galaxy with the baryon-dark border (dot line)

During the stream formation, the high-density region derived from the collision during the collapse spread out, so the density of the stream was too low to form stars. As the stream wrapped around at the center, the wrapping of the stream produces the high-density region for the star formation in a steady pace. Thus, the first stars and the black holes at the center in spiral galaxies are smaller than in elliptical galaxies. The stars at the

center became black holes and supernovas that induced the star formation in spiral arms. The massive center area decreases the angular speed around the center, greatly retarding the winding of the spiral arms around the center. With this steady pace, there are still many young stars in spiral galaxies. When there were more than one baryonic stream in the same general direction, there are more than two spiral arms.

Some streams went through the dark matter halos, and entered into the adjacent baryonic droplets. The adjacent droplet captured a part of the stream, and another part of the stream continued to move to the dark matter halo, and finally settled near the droplet in the dark matter halo. Dependent on the direction of the entry, the captured part of the stream later became a part of the disk of the host galaxy, star clusters in the halo, or both. The part of the stream that settled near the droplet became the dwarf spheroidal galaxy. Under continuous disruption and absorption of the tidal interaction from the large galaxy nearby, the dwarf spheroidal galaxy does not have well-defined baryonic-dark border, disk, and internal rotation.

When two connected dark matter cores inside far apart from each other (E in Fig. 9) generated two openings in opposite sides of the droplet, the momentum from the two opposite dark matter streams canceled each other nearly completely. The result was the slow moving baryonic droplet. Two opposite baryonic streams formed side by side with the two opposite dark matter streams. When the baryonic stream entered the dark matter halo, the size of the stream decreased due to the anti-expansion force by the dark matter, so there were the thick stream in the baryonic matter shell and the thin stream in the dark matter halo. As the baryonic stream penetrated into the dark matter halo, it met resistance from the strength of the baryon-dark border. Eventually, the stream stopped. The result after few differential rotations is the structure with one center, one bar from the thick stream stranding across the center, and arms attached to the bar as bar spiral galaxy as Fig. 11.

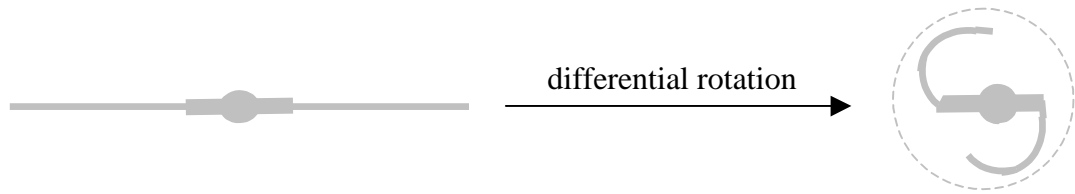


Fig. 11: from the distorted baryonic stream between the droplet and the halo to barred spiral galaxy with the baryon-dark border (dot line)

The result is barred spiral galaxy. As in normal spiral galaxy, the length of the spiral arm depends on the size of the dark matter core. The smallest dark matter core for barred spiral galaxy brings about SBa, and the largest dark matter core brings about SBd. The stars form in the low-density spiral arms much later than in the nucleus, so they are many young stars in the spiral arms.

If the size of the dark matter core was large (F in Fig. 9), the total dark matter mass was large enough for dark matter to have low droplet growth potential. The escape of the dark matter from the droplet involved little or no eruption, resulting in the gradual migration of large amount of dark matter outward and the gradual migration of small

amount of baryonic matter inward. Such opposite migrations are long and continuous processes. The result is irregular galaxy. When enough baryonic matter migrated to the center, and first star formation started. As baryonic matter continues migrating toward the center, the star formation continues in a slow rate up to the present time.

At the end of the big eruption, vast majority of baryonic matter was primordial free baryonic matter resided in dark matter outside of the galaxies from the big eruption. This free baryonic matter constituted the intergalactic medium (IGM). Stellar winds, supernova winds, and quasars provide heat and heavy elements to the IGM with ionized baryonic atoms. The heat prevented the formation of the baryonic droplet in the IGM.

Galaxies merged into new large galaxies, such as giant elliptical galaxy and cD galaxy ($z > 1-2$). Similar to the transient molecular cloud formation from the ISM (interstellar medium) through turbulence, the tidal debris and turbulence from the mergers generated the numerous transient molecular regions, which located in a broad area. The incompatibility between dark matter and baryonic matter transformed these transient molecular regions into the stable second-generation baryonic droplets surrounded by the dark matter halos. The baryonic droplets had much higher fraction of hydrogen molecules, much lower fraction of dark matter, higher density, and lower temperature, and lower entropy than the surrounding. The baryonic droplets started small with the enormous droplet growth potential. The rapid growth of the baryonic droplets drew large amount of the surrounding IGM inward, generating the IGM flow shown as the cooling flow. The IGM flow induced the galaxy flow. The IGM flow and the galaxy flow moved toward the merged galaxies, resulting in the protocluster ($z \sim 0.5$) with the merged galaxies as the cluster center.

Before the protocluster stage, spirals grew normally and passively by absorbing gas from the IGM as the universe expanded. During the protocluster stage ($z \sim 0.5$), the massive IGM flow injected a large amount of gas into the spirals that joined in the galaxy flow. Most of the injected hot gas passed through the spiral arms and settled in the bungle parts of the spirals. Such surges of gas absorption from the IGM flow resulted in major starbursts ($z \sim 0.4$) [16]. Meanwhile, the nearby baryonic droplets continued to draw the IGM, and the IGM flow and the galaxy flow continued. The results were the formation of high-density region, where the galaxies and the baryonic droplets competed for the IGM as the gas reservoir. Eventually, the maturity of the baryonic droplets caused a decrease in drawing the IGM inward, resulting in the slow IGM flow. Subsequently, the depleted gas reservoir could not support the major starbursts ($z \sim 0.3$). The galaxy harassment and the mergers in this high-density region disrupted the spiral arms of spirals, resulting in S0 galaxies with indistinct spiral arms ($z \sim 0.1 - 0.25$). The transformation process of spirals into S0 galaxies started at the core first, and moved to the outside of the core. Thus, the fraction of spirals decreases with decreasing distance from the cluster center [16].

The static and slow-moving baryonic droplets turned into dwarf elliptical galaxies and globular clusters. The fast moving baryonic droplets formed the baryonic stream. As the earlier baryonic stream during the big eruption, this baryonic stream underwent a differential rotation to minimize the interfacial area between the dark matter and baryonic matter. The result is the formation of blue compact dwarf galaxies (BCD), such as NGC

2915 with very extended spiral arms. Since the star formation is steady and slow, so the stars formed in BCD are new.

The galaxies formed during $z < 0.1$ -0.2 are mostly metal-rich tidal dwarf galaxies (TDG) from tidal tails torn out from interacting galaxies. In some cases, the tidal tail and the baryonic droplet merge to generate the starbursts with higher fraction of molecule than the TGD formed by tidal tail alone [17].

When the interactions among large galaxies were mild, the mild turbulence caused the formation of few molecular regions, which located in narrow area close to the large galaxies. Such few molecular regions resulted in few baryonic droplets, producing weak IGM flow and galaxy flow. The result is the formation of galaxy group, such as the Local Group, which has fewer dwarf galaxies and lower density environment than cluster.

Clusters merged to generate tidal debris and turbulence, producing the baryonic droplets, the ICM (intra-cluster medium) flow, and the cluster flow. The ICM flow and the cluster flow directed toward the merger areas among clusters and particularly the rich clusters with high numbers of galaxies. The ICM flow is shown as the warm filaments outside of cluster [18]. The dominant structural elements in superclusters are single or multi-branching filaments [19]. The cluster flow is shown by the tendency of the major axes of clusters to point toward neighboring clusters [20]. Eventually at the maximum incompatibility between dark matter and baryonic matter, the observable expanding universe will consist of giant voids and superclusters surrounded by the dark matter halos.

The whole observable expanding universe is the “Milky Universe” as one unit of emulsion with increasing incompatibility between dark matter and baryonic matter. The five periods of baryonic structure development are the free baryonic matter, the baryonic droplet, the galaxy, cluster, and the supercluster periods as Fig. 12. The first-generation galaxies are elliptical, normal spiral, barred spiral, irregular, and dwarf spheroidal galaxies. The second-generation galaxies are giant ellipticals, cD, evolved S0, dwarf ellipticals, BCD, and TDG. The universe now is in the early part of the supercluster period.

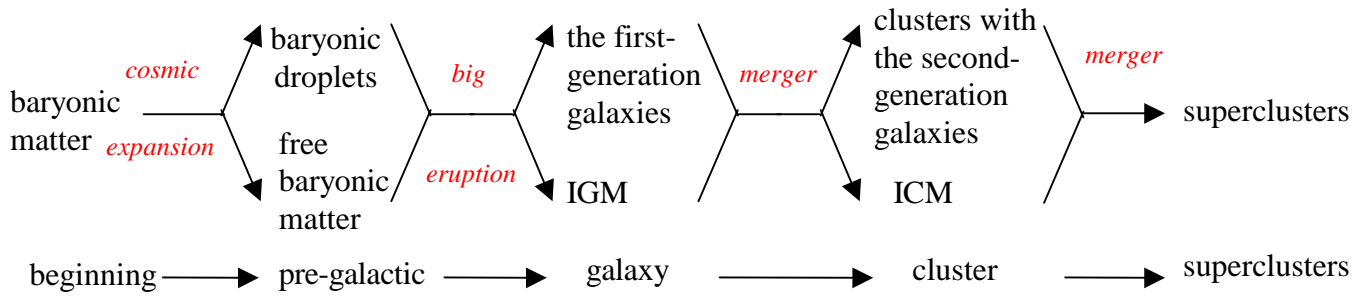


Fig. 12: the five levels of baryonic structure in the Milky Universe

6. The cyclic universe

The hidden universe is hidden from the observable universe until the hidden universe fractionalizes into mixed 3-particle, compatible with the empty mixed 3-particle

(exclusive vacuum overlapping with inclusive vacuum) in the observable universe. (With incompatible in physical laws, the two universes are still largely transparent to each other.) The empty mixed 3-particle from the observable universe and the mixed 3-particle from the hidden universe form the five dimensional bulk as in the two-sided Randall - Sundrum model [2] as Fig. 13.

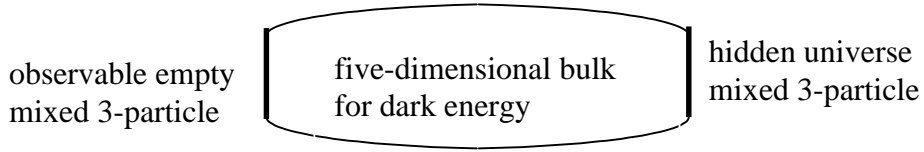


Fig. 13: compatible universes and dark energy

The five-dimensional bulk provides space for dark energy (quintessence) [21] as the scalar field from the hidden universe. When the hidden universe is in the fractionalization (expansion) phase from the mixed 4-particles to the mixed 3-particles, dark energy accelerates cosmic expansion in the observable universe.

After a certain period in the hidden universe, the mixed 3-particle starts to condense into the mixed 4-particle, inducing contraction in the observable universe. When all of the hidden universe mixed 3-particles is converted into the mixed 4-particles, the incompatible universes return, and dark energy ceases to exist.

Observations of quasars have strongly suggested [22] that the fine structure constant α at the present is slightly larger than α in the past. Martinez-Ledesma and Mendoza [23] suggested two fields, the “standard Maxwell’s field and a new scalar field. A generalized Lorentz force is expressed as $d\mathbf{P}/d\tau = \mathbf{F} \cdot \mathbf{J}_e + M \mathbf{J}_e$, where τ is the proper time and \mathbf{P} is the 1-form momentum, \mathbf{F} is the Maxwell 2-form field, \mathbf{J}_e is total current charge 1-form, and M is scalar field 0-form. The strength of M field is tiny to account for the tiny increase $\Delta\alpha$ of the fine structure constant. ($\Delta\alpha / \alpha = -0.72 \pm 0.18 \times 10^{-5}$) M field is the time dependent dark energy that relates to the time dependent compatibility between the hidden universe and the observable universe.

Dark energy controls the rate of expansion and contraction for the observable universe during the compatible universes period. It makes the hidden and the observable universes to have the same size and to contract at the same rate, so eventually both the observable universe and the hidden universe end at the same time.

At the end of the contraction, the hidden universe becomes the hidden mixed 9-particle, and the observable universe becomes a cosmic black hole without exclusive vacuum. Without exclusive vacuum, the cosmic black hole is converted back into the observable mixed 9-particle. Therefore, the universe has both sides of the mixed 9-particles as the mixed pre-expanding universe. This mixed pre-expanding universe then starts another cycle of the universe as Fig. 14.

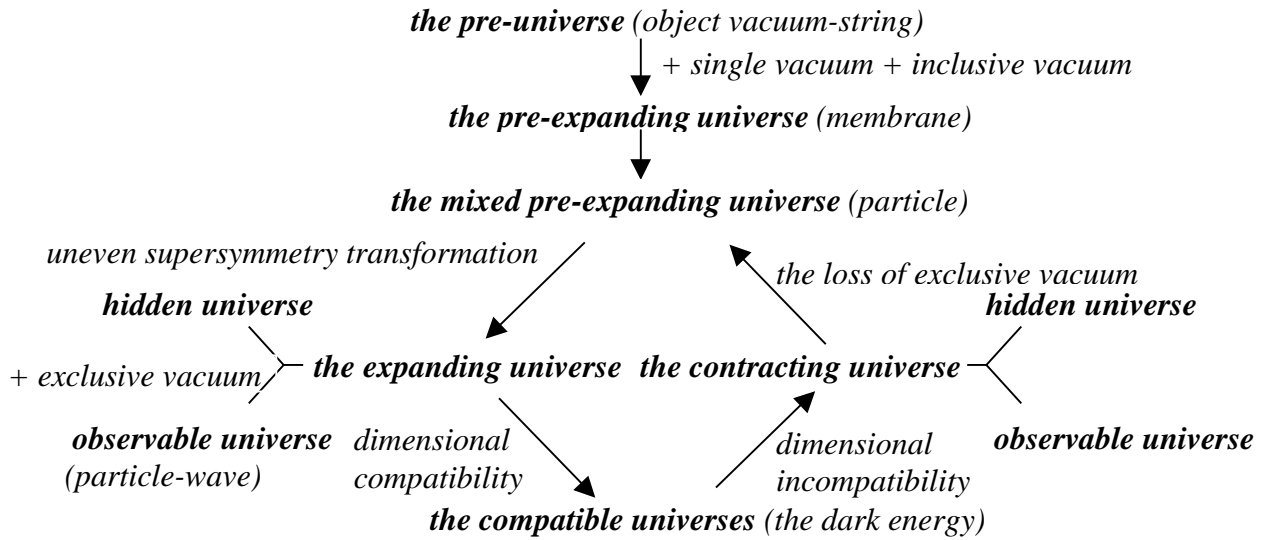


Fig. 14: the cyclic universe

7. *Quantum mechanics*

After the rupture, all four types of vacuum exist in all objects in the observable universe. The presence of object vacuum in object is manifested by the creation-annihilation of object. Inclusive vacuum and single vacuum exist complementarily in and around all matters, including both boson and fermion. In one inclusive vacuum, there are multiple objects, which can also be multiple states in one inclusive vacuum in one object, so inclusive vacuum fractionalizes an object into multiple states as wave, while single vacuum retains an object as single state as particle. The complementary existence of inclusive vacuum and single vacuum brings about the complementary principle between wave and particle.

Inclusive vacuum overlaps with exclusive vacuum surrounding a particle. In the overlapping space of inclusive vacuum and exclusive vacuum, various parts of the overlapping space undergo constant random changes from inclusion to exclusion and from exclusion to inclusion. The rate of change from inclusion to exclusion and from exclusion to inclusion is velocity. The requirement for randomness does not allow constant position and constant velocity (the rate of change) simultaneously. At an exact position, the variation in velocities is large. At an exact velocity, the variation in positions is large. The variation is uncertainty. This exclusion-inclusion of an object is essentially equivalent to subjective measurement of an object in Copenhagen interpretation of quantum mechanics. Therefore, the source of the uncertainty principle is subjective measurement or the objective exclusion. Consequently, an object has the probability to be anywhere in the form of wavefunction.

Exclusive vacuum is the gap between objects, so when two objects entangles (collides), exclusive vacuum disappears. During the entanglement, the original two sets of multiple states in inclusive vacuum no longer exist. By eliminating exclusive vacuum and inclusive vacuum, the entangled single vacuum with the one state, the entangled state, emerges. This is the collapse of wavefunction. Therefore, any measurement of wavefunction always ends with one state instead of multiple states. The summary is described in Fig. 15.

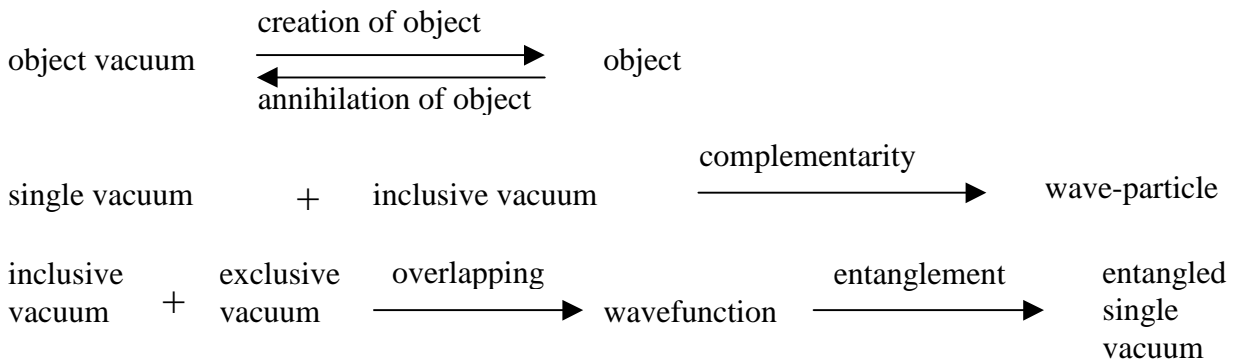


Fig. 15: quantum mechanics

8. *The force fields: the masses of gauge bosons*

In the observable universe, all four types of vacuum exist. Inclusive vacuum outside of a particle in the big bang mode allows all the mixed particles to have the same number of space dimensions. It is achieved by adding the virtual hierarchical space dimensions to inclusive vacuum surrounding the core mixed particles in the manner of the Kaluza-Klein structure. The virtual space dimensions are the space dimensions in between the core particle space dimension and the gravity (the eleventh space-time dimension). The masses of the hierarchical space dimensions follow the hierarchical dimensional mass formula as Eq. (3).

Since after the rupture, space dimension cannot be added or subtracted, the virtual hierarchical space dimensions have to be the same space dimension as the core particle. To provide the virtual hierarchical space dimensions with the same space-time dimension as the core mixed particle, the core mixed particle absorbs the virtual hierarchical dimensions as the scalar fields through Higgs mechanism. (There is no free Higgs boson. So far no free Higgs boson has been detected.) The surrounding virtual hierarchical dimensions are converted into the "dimensional orbitals" with the same space-time dimension as the core mixed particle. Gravity is a part of the dimensional orbitals shared by all mixed particles.

These hierarchical dimensional orbitals are the force and mass fields. The final forms of the mixed particles are the mixed particles from 3 to 9 surrounded by the hierarchical dimensional orbitals as the force and mass fields. Since the core mixed particles have two sets (main and auxiliary) of space dimensions, there are also two sets of the dimensional orbitals. For the mixed 3-particle (the mixture of leptons and quarks),

there are two sets (main and auxiliary) of the hierarchical seven dimensional orbitals (including gravity) and the non-hierarchical three core particle space dimensions. The total number of dimensional orbitals is 14 as shown in Fig. 16.

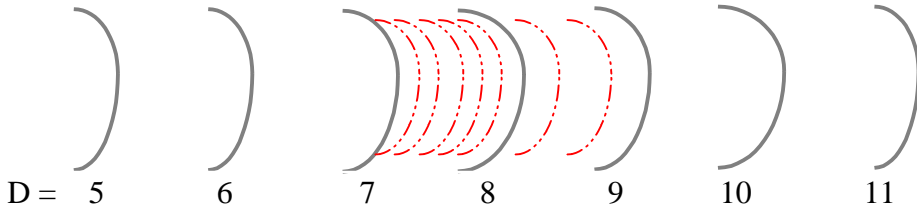


Fig. 16: 14 dimensional orbitals in the mixed 3-particle: 7 main dimensional orbitals (solid line), and 7 auxiliary dimensional orbitals (dot line), D = main dimensional orbital number

As shown in Fig. 16, the auxiliary dimensional orbitals are in the middle of the main dimensional orbitals.

The structure of the mixed 3-particle with dimensional orbitals resembles to the structure of atomic orbital. Consequently, the periodic table of elementary particles is constructed to account of all leptons, quarks, gauge bosons, and hadrons.

For the gauge bosons, the seven main dimensional orbitals are arranged as $F_5 B_5 F_6 B_6 F_7 B_7 F_8 B_8 F_9 B_9 F_{10} B_{10} F_{11} B_{11}$, where B and F are boson and fermion in each orbital. The masses of the main dimensional orbital bosons can be derived from Eqs. (1) and (2). Assuming $\alpha_{D,B} = \alpha_{D,F}$, the relation between the bosons in the adjacent main dimensional orbitals, then, can be expressed in terms of the main dimensional orbital number, D, as

$$M_{D-1,B} = M_{D,B} \alpha^2_D, \quad (4)$$

where $D=6$ to 11 , and $E_{5,B}$ and $E_{11,B}$ are the energies for the 5-main dimensional orbital and the 11-main dimensional orbital, respectively. The lowest energy is the Coulombic field,

$$E_{5,B} = \alpha M_{6,F} = \alpha M_e \quad (5)$$

The bosons generated are the main dimensional orbital bosons or B_D . Using only α_e , the mass of electron, the mass of Z^0 , and the number (seven) of dimensional orbitals, the masses of B_D as the gauge boson can be calculated as shown in Table 1.

Table 1. The Masses of the main dimensional orbital bosons:

$\alpha = \alpha_e$, $D = \text{main dimensional orbital number}$

B_D	M_D	GeV (calculated)	Gauge boson	Interaction, symmetry	Predecessor
B_5	$M_e \alpha$	3.7×10^{-6} (given)	A	Electromagnetic, $U(1)$	pre-charged
B_6	M_e/α	7×10^{-2}	$\pi_{1/2}$	Strong, $SU(3) \rightarrow U(1)$	pre-strong
B_7	$M_6/\alpha_w^2 \cos \theta_w$	91.177 (given)	Z_L^0	weak (left), $SU(2)_L$	Fractionalization
B_8	M_7/α^2	1.7×10^6	X_R	CP (right) nonconservation, $U(1)_R$ CP asymmetry	
B_9	M_8/α^2	3.2×10^{10}	X_L	CP (left) nonconservation, $U(1)_L$ CP asymmetry	
B_{10}	M_9/α^2	6.0×10^{14}	Z_R^0	weak (right), $SU(2)_R$	Fractionalization
B_{11}	M_{10}/α^2	1.1×10^{19}	G	gravity, D particle in $D+1$ bulk	Pregravity

In Table 1, $\alpha = \alpha_e$ (the fine structure constant for electromagnetic field), and α_w is not same as α of the rest, because as shown later, there is a mixing between B_5 and B_7 as the symmetry mixing between $U(1)$ and $SU(2)$ in the standard theory of the electroweak interaction, and $\sin \theta_w$ is not equal to 1. As shown later, B_5 , B_6 , B_7 , B_8 , B_9 , and B_{10} are A (massless photon), $\pi_{1/2}$, Z_L^0 , X_R , X_L , and Z_R^0 , respectively, responsible for the electromagnetic field, the strong interaction, the weak (left handed) interaction, the CP (right handed) nonconservation, the CP (left handed) nonconservation, and the P (right handed) nonconservation, respectively. The calculated value for θ_w is 29.69^0 in good agreement with 28.7^0 for the observed value of θ_w [24]. The calculated energy for B_{11} is 1.1×10^{19} GeV in good agreement with the Planck mass, 1.2×10^{19} GeV.

There are dualities between dimensional orbitals and the cosmic evolution. The pre-charged force, the pre-strong force, the fractionalization during the superluminal inflation, the CP asymmetry to generate matter during the rupture, and the pregravity are the predecessors of electromagnetic force, the strong force, the weak interaction, the CP nonconservation, and gravity, respectively. These forces are manifested in the main dimensional orbitals with various space-time symmetries and gauge symmetries. The strengths of these forces are different than their predecessors, and are arranged according to the dimensional orbitals. Each of the forces will be discussed as follows.

The pre-charged force is the predecessor of electromagnetism as the long-ranged force with the absorption-emission of massless particles with $U(1)$ symmetry. Being the main dimensional orbital with the lowest mass, B_5 is the utmost orbital, so as the utmost pre-charged force in the 10D X 1D Kaluza-Klein structure, electromagnetism is B_5 .

There is duality between the collapse of the pre-expanding universe and electromagnetism. The attraction between the 9-brane and the 9-antibrane is manifested as electric force. As the collapse of the pre-expanding universe begins, and the 9-brane and the 9-antibrane start to move, the attractive force and the repulsive force cause an inversion that turns the 9-brane and the 9-antibrane inside, and turns pregravity and the anti-

pregravity outside. In the observable universe, there is no repulsive force between pregravity and the anti-pregravity, so the force for the inversion is manifested as the force for the rotation, which is magnetic force, perpendicular to the direction of moving charging particles.

Only the mixed 3-particle (baryonic matter) has the B_5 , so without B_5 , dark matter consists of permanently neutral higher dimensional particles. It cannot emit light, cannot form atoms, and exists as neutral gas.

The short-ranged pre-strong force is the predecessor of the short-ranged strong force for quarks with the absorption-emission of massless particles through non-zero energy medium, pions. The pre-strong force is next to the pre-charged force, so the strong force for quarks is B_6 next to B_5 for electromagnetism. There is duality between B_6 and the hiding of quark as the auxiliary particle in the mixed 3-particle. Lepton is the main particle.

The hypercharges for both e^+ and ν are 1, while for both u and d quarks, they are 1/3. The electric charges for e^+ and ν are 1 and 0, respectively, while for u and d quarks, they are 2/3 and -1/3, respectively. The hiding of quark is achieved by the strong interaction for quark. The hiding is generated by "leptonization" [25], which means quarks have to behave like leptons in the main dimensional orbitals. Leptons have integer electric charges and hypercharges, while quarks have fractional electric charges and hypercharges. The leptonization is to make quarks behave like leptons in terms of "apparent" integer electric charges and hypercharges. There are two parts for this strong interaction: the first part is for the charge, and the second part is for the hypercharge. The first part of the strong interaction allows the combination of a quark and an antiquark in a particle, so there is no fractional electric charge. It involves the conversion of $\pi_{1/2}$ boson in B_6 into the electrically chargeless meson field by combining two $\pi_{1/2}$, analogous to the combination of e^+ and e^- fields, so the meson field becomes chargeless. (The mass of π , 135 MeV, is twice of the mass of a half-pion boson, 70 MeV, minus the binding energy. $\pi_{1/2}$ becomes pseudoscalar up or down quark in pion.) In the meson field, no fractional charge of quark can appear. The second part of the strong interaction is to combine three quarks in a particle, so there is no fractional hypercharge. It involves the conversion of B_5 ($\pi_{1/2}$) into the gluon field with three colors. The number of colors (three) in the gluon field is equal to the ratio between the lepton hypercharge and quark hypercharge. There are three $\pi_{1/2}$ in the gluon field, and at any time, only one of the three colors appears in a quark. Quarks appear only when there is a combination of all three colors or color-anticolor. In the gluon field, no fractional hypercharge of quarks can appear. By combining both of the meson field and the gluon field, the strong interaction is the three-color gluon field based on the chargeless vector meson field from the combination of two $\pi_{1/2}$'s. The total number of $\pi_{1/2}$ is 6, so the fine structure constant, α_s , for the strong force is

$$\begin{aligned} \alpha_s &= 6\alpha e^1 \\ &= 0.119 \end{aligned} \tag{6}$$

which is in a good agreement with the observed value, 0.124 [26]. Without colors, leptons do not have the strong force.

The fractionalization of the mixed particles during the superluminal inflation is the predecessor of the weak interaction for the changes of the flavors (masses) of particles. The two fractionalizations in the opposite sides (hidden and observable) of the expanding universe are chiral, so the weak interaction is chiral. The fractionalization involves the uneven supersymmetry transformation of a mixed particle into a lower dimensional and lower mass particle. In the weak interaction, gauge symmetry for the absorption and the emission of massive particle replaces the supersymmetry transformation that is no longer possible after the rupture. The method for such replacement is for the weak interaction to take part in the formation of electric charge, which involves the absorption and the emission of massless particle. It is the $U(1) \times SU(2)$ mixing to form electric charge. $U(1)$ is the non-fractionalization from the pre-electromagnetism, so assign hypercharge of 1 to both pre- e^+ and pre- ν , respectively. In $SU(2)$, pre- e^+ and pre- ν are before and after the fractionalization, respectively, so assign isospin 1/2 and -1/2 to pre- e^+ and pre- ν , respectively. The mixing of $U(1)$ and $SU(2)$ leads to electric charge = hypercharge/2 + isospin. The electric charges of e^+ and ν are equal to 1 and 0, respectively.

B_7 carries the charge for the gauge symmetry for the weak interaction within the family of leptons or quarks at different dimensional orbitals. There is the mixing between B_5 and B_7 , corresponding to the $U(1) \times SU(2)$ mixing. The absolute or nearly absolute chiral symmetry (permanent chirality) generates massless or nearly massless neutrinos.

The CP asymmetry to generate matter during the rupture is the predecessor of the CP nonconservation that is B_9 for CP (left) with $U(1)$ symmetry. For the reason of symmetry, P and CP nonconservations are in pairs of the right and the left. B_7 , B_8 , B_9 , and B_{10} carry P (left), CP (right), CP (left), and P (right) nonconservation, respectively. However, only P (left) at B_7 and CP (left) at B_9 relate to the fractionalization and the CP asymmetry to generate matter, respectively, in the observable universe.

The dimensional boson, B_8 , is a CP (right). The ratio of the force constants between the CP-invariant W_L in B_8 and the CP-violating X_R in B_8 is

$$\begin{aligned} \frac{G_8}{G_7} &= \frac{\alpha E_7^2 \cos^2 \Theta_W}{\alpha_W E_8^2} \\ &= 5.3 \times 10^{-10} , \end{aligned} \tag{7}$$

which is in the same order as the ratio of the force constants between the CP-invariant weak interaction and the CP-violating interaction with $|\Delta S| = 2$. The B_8 does not generate matter.

The dimensional boson, B_9 (X_L), has the CP-violating $U(1)_L$ symmetry. B_9 generates matter. As shown in Fig. 17, the lepton (l_9) and the quark (q_9) are outside of the three families for leptons and quarks, so baryons in dimension nine do not have to have the baryon number conservation. The baryon that does not conserve baryon number has the baryon number of zero. The combination of the CP-nonconservation and the baryon number of zero leads to the baryon, \bar{p}_9^- , with the baryon number of zero and the baryon, p_9^+ , with the

baryon number of 1. The decay of the baryon \bar{p}_9^- with zero baryon number into the leptons, whose sum of lepton numbers is zero, is as follows.

$$\bar{p}_9^- \rightarrow l_9^- \bar{l}_9^\circ$$

The combination this \bar{p}_9^- and p_9^+ as well as leptons $l_9^\circ \bar{l}_9^\circ$ and gauge boson X_L results in

$$\begin{aligned} p_9^+ \bar{p}_9^- + l_9^\circ \bar{l}_9^\circ &\xrightarrow{X_L} p_9^+ + l_9^- \bar{l}_9^\circ + l_9^\circ \bar{l}_9^\circ \\ &\rightarrow p_9^+ + l_9^- + \text{radiation} + \bar{l}_9^\circ \\ &\rightarrow n_9^\circ + \text{radiation} \end{aligned}$$

Consequently, excess baryons, n_9° , are generated in the dimension nine. These excess baryons, n_9° , become the predecessors of excess neutrons in the low energy level.

The ratio of force constants between X_R with CP conservation and X_L with CP-nonconservation is

$$\begin{aligned} \frac{G_9}{G_8} &= \frac{\alpha E_8^2}{\alpha E_9^2} \\ &= 2.8 \times 10^{-9} \quad , \end{aligned} \tag{8}$$

which is the ratio of the numbers between matter (dark and baryonic) and photons in the universe. The mass of baryonic matter is 1/8 of the total mass of matter, and the number of baryonic matter is approximately 1/3 to 1/4 of the total number of matter. Hence, the ratio of the numbers between baryonic matter and photons is about 7 to 9×10^{-10} , which is close to the ratio (around 5×10^{-10}) obtained by the big bang nucleosynthesis.

Gravity, the individualized pregravity, continues to have the same long-ranged force with the Planck-infinite dimension as pregravity. Therefore, gravity continues to be B_{11} with the Planck mass. The summary of all forces and their predecessors is in Table 1.

9. The periodic table of elementary particles: the masses of leptons and quarks

The two sets of seven dimensional orbitals result in 14 dimensional orbitals (Fig. 17) for gauge bosons, leptons, and quarks. The periodic table for elementary particles is shown in Table 2.

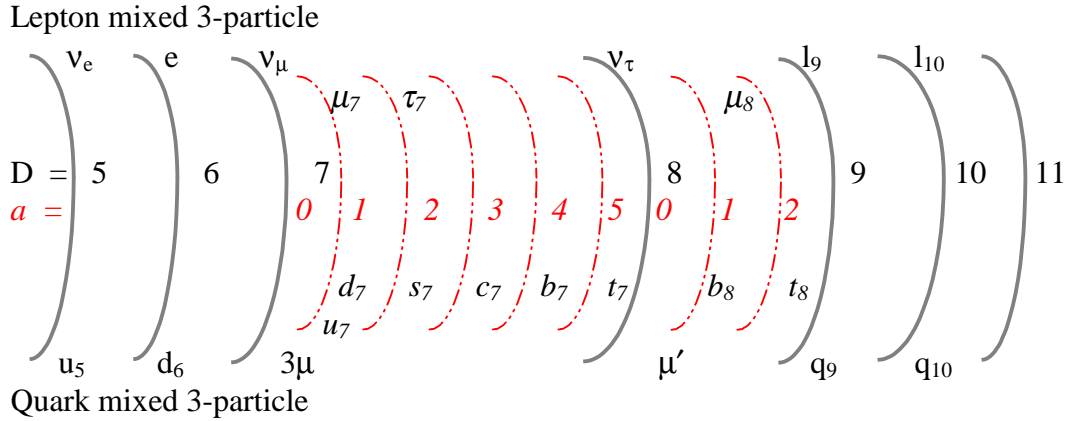


Fig. 17: leptons and quarks in the dimensional orbits
 $D =$ main dimensional orbital number, $a =$ auxiliary dimensional orbital number

Table 2. The Periodic Table of elementary particles

$D =$ main dimensional orbital number, $a =$ auxiliary dimensional orbital number

D	$a = 0$	1	2	$a = 0$	1	2	3	4	5
<u>Lepton</u>									
5	$l_5 = v_e$			$q_5 = u_5 = 3v_e$					$B_5 = A$
6	$l_6 = e$			$q_6 = d_6 = 3e$					$B_6 = \pi_{1/2}$
7	$l_7 = v_\mu$	μ_7	τ_7	$q_7 = 3\mu$	u_7/d_7	s_7	c_7	b_7	t_7
8	$l_8 = v_\tau$	μ_8		$q_8 = \mu'$	b_8	t_8			$B_8 = X_R$
9	l_9			q_9					$B_9 = X_L$
10	f_{10}								$B_{10} = Z_R^0$
11	f_{11}								$B_{11} = G$
<u>Quark</u>									
<u>Boson</u>									

D is the dimensional orbital number for the seven main dimensional orbitals. The auxiliary dimensional orbital number, a , is for the seven extra auxiliary dimensional orbitals. All gauge bosons, leptons, and quarks are located on the seven main dimensional orbits and seven auxiliary orbits. v_e , e , v_μ , and v_τ are main dimensional fermions for main dimension 5, 6, 7, and 8, respectively. All neutrinos have zero mass because of chiral symmetry (permanent chirality).

The dimensional fermions for $D = 5$ and 6 are neutrino (l_5) and electron (l_6), respectively. To generate a quark whose mass is higher than the lepton is to add the lepton to the boson from the combined lepton-antilepton, so the mass of the quark is three times of the mass of the corresponding lepton in the same main dimension. The equation for the quark mass is

$$M_{q_D} = 3M_{l_D} \quad (9)$$

A heavy lepton (μ or τ) is the combination of the dimensional leptons and the auxiliary dimensional leptons. In the same way, a heavy quark is the combination of the dimensional quarks from Eq.(9) and the auxiliary quarks. The mass of the auxiliary dimensional fermion (AF for both heavy lepton and heavy quark) is generated from the corresponding main dimensional boson as follows.

$$M_{AF_{D,a}} = \frac{M_{B_{D-1,0}}}{\alpha_a} \sum_{a=0}^a a^4 \quad , \quad (10)$$

where α_a = auxiliary dimensional fine structure constant, and a = auxiliary dimension number = 0 or integer. The first term, $\frac{M_{B_{D-1,0}}}{\alpha_a}$, of the mass formula (Eq. (10)) for the auxiliary dimensional fermions is derived from the mass equation, Eq. (1), for the dimensional fermions and bosons. The second term, $\sum_{a=0}^a a^4$, of the mass formula is for Bohr-Sommerfeld quantization for a charge - dipole interaction in a circular orbit as described by A. Barut [27]. $1/\alpha_a$ is 3/2. The coefficient, 3/2, is to convert the main dimensional boson mass to the mass of the auxiliary dimensional fermion in the higher dimension by adding the boson mass to its fermion mass which is one-half of the boson mass. The formula for the mass of auxiliary dimensional fermions (AF) becomes

$$\begin{aligned} M_{AF_{D,a}} &= \frac{M_{B_{D-1,0}}}{\alpha_a} \sum_{a=0}^a a^4 \\ &= \frac{3}{2} M_{B_{D-1,0}} \sum_{a=0}^a a^4 \\ &= \frac{3}{2} M_{F_{D,0}} \alpha_D \sum_{a=0}^a a^4 \end{aligned} \quad (11)$$

When the mass of this auxiliary dimensional fermion is added to the sum of masses from the corresponding main dimensional fermions (zero auxiliary dimension number) with the same electric charge and the same main dimension, the fermion mass formula for heavy leptons and quarks is derived as follows.

$$\begin{aligned} M_{F_{D,a}} &= \sum M_{F_{D,0}} + M_{AF_{D,a}} \\ &= \sum M_{F_{D,0}} + \frac{3}{2} M_{B_{D-1,0}} \sum_{a=0}^a a^4 \\ &= \sum M_{F_{D,0}} + \frac{3}{2} M_{F_{D,0}} \alpha_D \sum_{a=0}^a a^4 \end{aligned} \quad (12)$$

Each fermion can be defined by main dimensional numbers (D's) and auxiliary dimensional numbers (a's). Heavy leptons and quarks consist of one or more D's and a's. The compositions and calculated masses of leptons and quarks are listed in Table 3.

Table 3. The Compositions and the Constituent Masses of Leptons and Quarks
D = main dimensional orbital number and a = auxiliary dimensional orbital number

	D _a	Composition	Calc. Mass
<u>Leptons</u>	<u>D_a for leptons</u>		
v _e	5 ₀	v _e	0
E	6 ₀	E	0.51 MeV (given)
v _μ	7 ₀	v _μ	0
v _τ	8 ₀	v _τ	0
μ	6 ₀ + 7 ₀ + 7 ₁	e + v _μ + μ ₇	105.6 MeV
τ	6 ₀ + 7 ₀ + 7 ₂	e + v _μ + τ ₇	1786 MeV
<u>Quarks</u>	<u>D_a for quarks</u>		
U	5 ₀ + 7 ₀ + 7 ₁	u ₅ + q ₇ + u ₇	330.8 MeV
D	6 ₀ + 7 ₀ + 7 ₁	d ₆ + q ₇ + d ₇	332.3 MeV
S	6 ₀ + 7 ₀ + 7 ₂	d ₆ + q ₇ + s ₇	558 MeV
C	5 ₀ + 7 ₀ + 7 ₃	u ₅ + q ₇ + c ₇	1701 MeV
B	6 ₀ + 7 ₀ + 7 ₄	d ₆ + q ₇ + b ₇	5318 MeV
T	5 ₀ + 7 ₀ + 7 ₅ + 8 ₀ + 8 ₂	u ₅ + q ₇ + t ₇ + q ₈ + t ₈	176.5 GeV

The lepton for main dimension five is v_e, and the quark for the same main dimension is u₅, whose mass is equal to 3 Mv_e from Eq. (9). The lepton for the main dimension six is e, and the quark for this main dimension is d₆. u₅ and d₆ represent the “light quarks” or “current quarks” which have low masses. The main dimensional lepton for the dimensions seven is v_μ. All v's become massless by the chiral symmetry to preserve chirality. The auxiliary dimensional leptons (Al) in the main dimension seven are μ₇ and τ₇ whose masses can be calculated by Eq. (13) derived from Eq. (11).

$$\begin{aligned}
 M_{Al_{7,a}} &= \frac{3}{2} M_{B_{6,0}} \sum_{a=0}^a a^4 \\
 &= \frac{3}{2} M_{\pi_{l/2}} \sum_{a=0}^a a^4 \quad ,
 \end{aligned} \tag{13}$$

where a = 1, 2 for μ₇ and τ₇, respectively.

For heavy quarks, q_7 (the main dimensional fermion, F_7 , for quarks in the main dimension seven) is 3μ instead of massless $3v$ as in Eq. (9). According to the mass formula, Eq. (11), of the auxiliary fermion, the mass formula for the auxiliary quarks, $Aq_{7,a}$, is as follows.

$$\begin{aligned} M_{Aq_{7,a}} &= \frac{3}{2} M_{q_7} \alpha_7 \sum_{a=0}^a a^4 \\ &= \frac{3}{2} (3 M_\mu) \alpha_w \sum_{a=0}^a a^4 \quad , \end{aligned} \tag{14}$$

where $\alpha_7 = \alpha_w$, and $a = 1, 2, 3, 4$, and 5 for $u_7/d_7, s_7, c_7, b_7$, and t_7 , respectively.

The main dimensional lepton for the main dimension eight is v_τ , whose mass is zero to preserve chirality. The heavy lepton for the main dimensional eight is μ' as the sum of e , μ , and μ_8 (auxiliary dimensional lepton). Because there are only three families for leptons, μ' is the extra lepton, which is "hidden". μ' can appear only as $\mu + \text{photon}$. The pairing of $\mu + \mu$ from the hidden μ' and regular μ may account for the occurrence of same sign dilepton in the high energy level [28]. For the main dimension eight, q_8 (the F_8 for quarks) is μ' instead of $3\mu'$, because the hiding of μ' allows q_8 to be μ' . The hiding of μ' for leptons is balanced by the hiding of b_8 for quarks. The calculated masses are in good agreement with the observed constituent masses of leptons and quarks [29] [30]. The observed mass of the top quark is 174.3 ± 5.1 GeV [30] in a good agreement with the calculated value, 176.5 GeV. The masses of leptons, quarks, gauge bosons, and hadrons are calculated with only four known constants: the number of spatial dimensions, the mass of electron, the mass of Z° , and α_e .

10. The masses of hadrons

As molecules are the composites of atoms, hadrons are the composites of elementary particles. Hadron can be represented by elementary particles in many different ways. One way to represent hadron is through the nonrelativistic constituent quark model where the mass of a hadron is the sum of the masses of quarks plus a relatively small binding energy. $\pi_{1/2}$ (u or d pseudoscalar quark), u, d, s, c, b, and t quarks mentioned above are nonrelativistic constituent quarks. On the other hand, except proton and neutron, all hadrons are unstable, and decay eventually into low-mass quarks and leptons. Is a hadron represented by all nonrelativistic quarks or by low-mass quarks and leptons? This paper proposes a dual formula: the full quark formula for all nonrelativistic constituent quarks ($\pi_{1/2}$, u, d, s, c, and b) and the basic fermion formula for the lowest- mass quark ($\pi_{1/2}$ and u) and lepton (e). The calculation of the masses of hadrons requires both formulas. The full quark formula sets the initial mass for a hadron. This initial mass is matched by the mass resulted from the combination of various particles in the basic fermion formula. The mass of a hadron is the mass of the basic fermion formula plus the binding energy (negative energy).

$$M_{\text{full quark formula}} \approx M_{\text{basic fermion formula}}$$

$$M_{\text{hadron}} = M_{\text{basic fermion formula}} + \text{binding energy} \quad (15)$$

This dual representation of hadrons by the full quark formula and the basic quark formula is seen in the treatment of nucleons [31] as a mixture of the quark model and the vector meson dominance model which can be represented by $\pi_{1/2}$ and u .

The full quark formula consists of the vector quarks (u , d , s , c , and b) and pseudoscalar quark, $\pi_{1/2}$ (70.03 MeV), which is B_6 (dimension boson in the dimension six). The strong interaction converts B_6 ($\pi_{1/2}$) into pseudoscalar u and d quark in pseudoscalar π meson. The combination of the pseudoscalar quark ($\pi_{1/2}$) and vector quarks (q) results in hybrid quarks (q') whose mass is the average mass of pseudoscalar quark and vector quark.

$$M_{q'} = 1/2 (M_q + M_{\pi_{1/2}}) \quad (16)$$

Hybrid quarks include u' , d' , and s' whose masses are 200.398, 201.164, and 314.148 MeV, respectively. For baryons other than n and p , the full quark formula is the combination of vector quarks, hybrid quarks (u' and d'), and pseudoscalar quark ($\pi_{1/2}$). For example, Λ° (uds) is $u'd's3$, where 3 denotes 3 $\pi_{1/2}$. For pseudoscalar mesons ($J = 0$), the full quark formula is the combination of $\pi_{1/2}$ and q' (u' , d' and s') or $\pi_{1/2}$ alone. For vector mesons ($J > 0$), the full quark formula is the combination of vector quarks (u , d , s , c , and b) and $\pi_{1/2}$. For examples, π° is 2, η (1295, $J=0$) is $u'u'd'd'8$, and K_1 (1400, $J=1$) is $ds8$. The compositions of hadrons from the particles of the full quark formula are listed in Table 4.

Table 4. Particles for the full quark formula

	$\pi_{1/2}$	u', d'	s'	u, d	s	c, b
mass (MeV) (from Tables 1 and 3 and Eq. (16))	70.025	200.40, 201.16	314.15	330.8, 332.3	558	1701, 5318
n and p					✓	
Baryons other than n and p	✓	✓			✓	✓
Mesons ($J = 0$) except $c\bar{c}$ and $b\bar{b}$	✓	✓	✓			✓
Mesons ($J > 0$) and $c\bar{c}$ and $b\bar{b}$	✓			✓	✓	✓

Different energy states in hadron spectroscopy are the results of differences in the numbers of $\pi_{1/2}$. The higher the energy state, the higher the number of $\pi_{1/2}$. The number of $\pi_{1/2}$ attached to q or q' in the full quark formula is restricted. The number of $\pi_{1/2}$ can be $0, \pm 1, \pm 3, \pm 4, \pm 7$, and $\pm 3n$ ($n > 2$). This is the “ $\pi_{1/2}$ series.” The number, 3, is indicative of a baryon-like (3 quarks in a baryon) number. The number, 4, is the combination of 1 and 3, while the number, 7, is the combination of 3 and 4. Since $\pi_{1/2}$ is essentially pseudoscalar u

and d quarks, the $\pi_{1/2}$ series is closely related to u and d quarks. Since s is close to u and d, the $\pi_{1/2}$ series is also related to s quark. Each presence of u, d, and s associates with one single $\pi_{1/2}$ series. The single $\pi_{1/2}$ series associates with baryons and the mesons with $u \bar{u}$, $d \bar{d}$, $s \bar{s}$, $d \bar{s}$, $s \bar{d}$, $d \bar{c}$, $u \bar{c}$, $d \bar{b}$, $u \bar{b}$, $s \bar{c}$, and $s \bar{b}$. The combination of two single $\pi_{1/2}$ series is the double $\pi_{1/2}$ series (0, ± 2 , ± 6 , ± 8 , ± 14 , and $\pm 6n$) associating with $u \bar{d}$ and $d \bar{s}$ mesons. For the mesons ($c \bar{c}$ and $b \bar{b}$) without u, d, or s, the numbers of $\pi_{1/2}$ attached to quarks can be from the single $\pi_{1/2}$ series or the double $\pi_{1/2}$ series.

The basic fermion formula is similar to M. H. MacGregor's light quark model [32], whose calculated masses and the predicted properties of hadrons are in very good agreement with observations. In the light quark model, the mass building blocks are the "spinor" (S with mass 330.4 MeV) and the mass quantum (mass = 70 MeV). For the basic fermion formula, S is u, the quark with the lowest mass (330.77 MeV), and the basic quantum is $\pi_{1/2}$ (mass = 70.025 MeV). For examples, in the basic fermion formula, neutron is SSS, and K_1 (1400, $J=1$) is $S_2 11$, where S_2 denotes two S, and 11 denotes 11 $\pi_{1/2}$'s.

In addition to S and $\pi_{1/2}$, the basic fermion formula includes P (positive charge) and N (neutral charge) with the masses of proton and neutron. As in the light quark model, the mass associated with positive or negative charge is the electromagnetic mass, 4.599 MeV, which is nine times the mass of electron. This mass (nine times the mass of electron) is derived from the baryon-like electron that represents three quarks in a baryon and three electrons in d_6 quark as in Table 2. This electromagnetic mass is observed in the mass difference between π^0 (2) and π^+ (2+) where + denotes positive charge. The calculated mass difference is one electromagnetic mass, 4.599 MeV, in good agreement with the observed mass difference, 4.594 MeV, between π^0 and π^+ . (The values for observed masses are taken from "Particle Physics Summary" [30].) The particles in the basic fermion formula are listed in Table 5.

Table 5. Particles in the basic fermion formula

S	$\pi_{1/2}$	N	P	electromagnetic mass
mass (MeV) 330.77	70.0254	939.565	938.272	4.599

Hadrons are the composites of quarks as molecules composing of atoms. As atoms are bounded together by chemical bonds, hadrons are bounded by "hadronic bonds," connecting the particles in the basic fermion formula. These hadronic bonds are similar to the hadronic bonds in the light quark model.

The hadronic bonds are the overlappings of the auxiliary dimensional orbits. As in Eq (11), the energy derived from the auxiliary orbit for S (u quark) is

$$\begin{aligned} E_a &= (3/2) (3 M_\mu) \alpha_w \\ &= 14.122 \text{ MeV} \end{aligned} \tag{17}$$

The auxiliary orbit is a charge - dipole interaction in a circular orbit as described by A. Barut [27], so a fermion for the circular orbit and an electron for the charge are embedded in this hadronic bond. The fermion for the circular orbit is the supersymmetry fermion for the auxiliary dimensional orbit according to Eq (2).

$$M_f = E_a \alpha_w \quad (18)$$

The binding energy (negative energy) for the bond (S–S) between two S's is twice of 14.122 MeV minus the masses of the supersymmetry fermion and electron.

$$\begin{aligned} E_{S-S} &= -2(E_a - M_f - M_e) \\ &= -26.384 \text{ MeV} \end{aligned} \quad (19)$$

It is similar to the binding energy (-26 MeV) in the light quark model. An example of S–S bond is in neutron (S – S – S) which has two S – S bonds. The mass of neutron can be calculated as follows.

$$\begin{aligned} M_n &= 3M_S + 2E_{S-S} \\ &= 939.54 \text{ MeV}, \end{aligned} \quad (20)$$

which is in excellent agreement with the observed mass, 939.57 MeV. The mass of proton is the mass of neutron minus the mass difference (three times of electron mass = M_{3e}) between u and d quark as shown in Table 2. Proton is represented as S – S – (S -3e). The calculation of the mass of proton is as follows.

$$\begin{aligned} E_a \text{ for } (S-3e) &= (3/2)(3(M_\mu - M_{3e})) \alpha_w \\ M_f &= E_a \alpha_w \\ M_p &= 2M_S + M_{(S-3e)} + E_{S-S} + E_{S-(S-3e)} \\ &= 938.21 \text{ MeV} \end{aligned} \quad (21)$$

The calculated mass is in a good agreement with the observed mass, 938.27 MeV.

The binding energy for $\pi_{1/2} - \pi_{1/2}$ bond can be derived in the same way as Eqs (17), (18), and (19).

$$\begin{aligned} E_a &= (3/2) M \pi_{1/2} \alpha_w \\ M_f &= E_a \alpha_w \\ E \pi_{1/2} - \pi_{1/2} &= -2(E_a - M_f - M_e) \\ &= -5.0387 \text{ MeV} \end{aligned} \quad (22)$$

It is similar to the binding energy (-5 MeV) in the light quark model. An example for the binding energy of $\pi_{1/2} - \pi_{1/2}$ bond is in π° . The mass of π° can be calculated as follows.

$$\begin{aligned} M_{\pi^\circ} &= 2M \pi_{1/2} + E \pi_{1/2} - \pi_{1/2} \\ &= 135.01 \text{ MeV}. \end{aligned} \quad (23)$$

The calculated mass of π^0 is in excellent agreement with the observed value, 134.98 MeV. There is one $\pi_{1/2} - \pi_{1/2}$ bond per pair of $\pi_{1/2}$'s, so there are two $\pi_{1/2} - \pi_{1/2}$ bonds for 4 $\pi_{1/2}$'s, and three $\pi_{1/2} - \pi_{1/2}$ bonds for 6 $\pi_{1/2}$'s.

Another bond is $N - \pi_{1/2}$ or $P - \pi_{1/2}$, the bond between neutron or proton and $\pi_{1/2}$. Since N is SSS , $N - \pi_{1/2}$ bond is derived from $S - \pi_{1/2}$. The binding energy of $S - \pi_{1/2}$ is the average between $S - S$ and $\pi_{1/2} - \pi_{1/2}$.

$$E_{S - \pi_{1/2}} = 1/2 (E_{S-S} + E_{\pi_{1/2} - \pi_{1/2}}) \quad (24)$$

An additional dipole (e^+e^-) is needed to connect $S - \pi_{1/2}$ to neutron.

$$\begin{aligned} E_{N - \pi_{1/2}} &= E_{S - \pi_{1/2}} + 2 M_e \\ &= -14.689 \text{ MeV}. \end{aligned} \quad (25)$$

It is similar to -15 MeV in the light quark model. An example for $P - \pi_{1/2}$ is Σ^+ which is represented by P4 whose structure is $2 - P - 2$. The 4 $\pi_{1/2}$'s are connected to P with two $P - \pi_{1/2}$ bonds. The mass of Σ^+ is as follows.

$$\begin{aligned} M_{\Sigma^+} &= M_P + 4 M_{\pi_{1/2}} + 2 E_{N - \pi_{1/2}} \\ &= 1189.0 \text{ MeV}. \end{aligned} \quad (26)$$

The calculated mass is in a good agreement with the observed mass, 1189.4 ± 0.07 MeV.

There is $N - N$ hadronic bond between two N 's. N has the structure of $S - S - S$. $N - N$ has a hexagonal structure shown in Fig. 18.

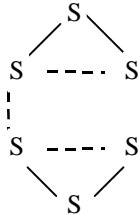


Fig. 18 The structure of $N - N$

There are two additional $S - S$ for each N . The total number of $S - S$ bonds between two N 's is 4. An example is Ω^0_c (ssc) which has the basic fermion formula of $N_2 S9$ with the structure of $3 - N - N - 6 S$. The mass of Ω^0_c can be calculated as follows.

$$\begin{aligned} M_{\Omega^0_c} &= 2M_N + M_S + 9M_{\pi_{1/2}} + 4 E_{S-S} + 2 E_{N - \pi_{1/2}} \\ &= 2705.3 \text{ MeV} \end{aligned} \quad (27)$$

The calculated mass for Ω^0_c is in a good agreement with the observed mass (2704 ± 4 MeV). For baryons other than p and n, there are two or three $N - \pi_{1/2}$ or $P - \pi_{1/2}$ bonds per baryon. It is used to distinguish $J = 1/2$ and $J \geq 3/2$. For $J = 1/2$ which have asymmetrical

spins (two up and one down), there are two bonds for three S in a baryon to represent the asymmetrical spins. For $J \geq 3/2$, there are three bonds for three S in a baryon except if there is only one $\pi_{1/2}$, only two bonds exists for a baryon.

Among the particles in the basic fermion formula, there are hadronic bonds, but not all particles have hadronic bonds. In the basic fermion formula, hadronic bonds appear only among the particles that relate to the particles in the corresponding full quark formula. The related particles are the “core” particles that have hadronic bonds, and the unrelated particles are “filler” particles that have no hadronic bonds. In the basic fermion formula, for baryons other than p and n, the core particles are P, N, and $\pi_{1/2}$. For the mesons consisting of u and d quarks, the core particles are $\pi_{1/2}$, S, and N. For the mesons containing one u, d, or s along with s, c, or b, the core particles are S and N, and no hadronic bond exist among $\pi_{1/2}$ ’s, which are the filler particles. For the mesons ($c\bar{c}$ and $b\bar{b}$), the only hadronic bond is N – N. The occurrences of hadronic bonds are listed in Table 6.

Table 6. Hadronic bonds in hadrons

	S – S	$\pi_{1/2} - \pi_{1/2}$	N(P) - $\pi_{1/2}$	N – N
Binding energy (MeV)	-26.384	-5.0387	-14.6894	2 S–S per N
Baryons other than n and p	✓		✓	✓
Mesons with u and d only	✓	✓		✓
Mesons containing one u, d, or s along with s, c, or b $c\bar{c}$ or $b\bar{b}$ mesons	✓		✓	✓

An example is the difference between π and f_0 . The decay modes of f_0 include the mesons of s quarks from K meson. Consequently, there is no $\pi_{1/2} - \pi_{1/2}$ for f_0 . The basic fermion formula for f_0 is 14. The mass of f_0 is as follows.

$$\begin{aligned} M &= 14M\pi_{1/2} \\ &= 980.4 \text{ MeV} \end{aligned} \tag{28}$$

The observed mass is 980 ± 10 MeV.

In additional to the binding energies for hadronic bonds, hadrons have Coulomb energy (-1.2 MeV) between positive and negative charges and magnetic binding energy (± 2 MeV per interaction) for S – S from the light quark model [32]. In the light quark model, the dipole moment of a hadron can be calculated from the magnetic binding energy. Since in the basic fermion formula, magnetic binding energy becomes a part of hadronic binding energy as shown in Eq (19), magnetic binding energy for other baryons is the difference in magnetic binding energy between a baryon and n or p. If a baryon has a similar dipole moment as p or n, there is no magnetic binding energy for the baryon. An example for Coulomb energy and magnetic binding energy is Λ (uds, $J=1/2$) whose formula is P3- with the structure of 2 – P – 1- where “-” denotes negative charge. The

dipole moment of Λ is $-6.13 \mu_N$, while the dipole moment of proton (P) is $2.79 \mu_N$ [32]. According to the light quark model, this difference in dipole moment represents -6 MeV magnetic binding energy. The Coulomb energy between the positive charge P and the negative charge 1- is -1.2 MeV . The electromagnetic mass for 1- is 4.599 MeV . The mass of Λ is calculated as follows.

$$\begin{aligned} M_\Lambda &= M_P + 3M\pi_{1/2} + M_{e.m.} + 2 E_{N-\pi_{1/2}} + E_{mag} + E_{coul} \\ &= 1116.4 \text{ MeV} \end{aligned} \quad (29)$$

The observed mass is $1115.7 \pm 0.0006 \text{ MeV}$.

An example of the dual representation of the full quark formula and the basic fermion formula as expressed by Eq. (15) is Λ (uds). The full quark formula for Λ is $u'd's'3$ with mass of 1169.9 MeV . This mass is matched by the mass of the basic fermion formula, $P3-$ with the mass of 1152.9 MeV . The final mass of Λ is 1152.9 MeV plus the various binding energies.

Table 7 is the results of calculation for the masses of baryons selected from Ref. [30]. The hadrons selected are the hadrons with precise observed masses and precise known quantum states such as isospin, spin, and decay mode.

Table 7. The masses of baryons

Baryons	$I(J^P)$	Full quark formula	Basic fermion formula	Calculated mass	Observed mass	Difference
<u>n and p</u>						
N	$1/2(1/2^+)$	Udd	SSS	939.54	939.57	-0.03
P	$1/2(1/2^+)$	Uud	SSS-3e	938.21	938.27	-0.06
<u>uds, uus, dds</u>						
Λ^0	$0(1/2^+)$	U'd's3	P3-	1116.4	1115.7	0.7
Σ^+	$1(1/2^+)$	U'u's4	P4	1189.0	1189.4	-0.4
Σ^0	$1(1/2^+)$	U'd's4	P4-	1192.4	1192.6	-0.2
Σ^-	$1(1/2^+)$	D'd's4	N4-	1194.9	1197.4	-2.5
Σ^+	$1(3/2^+)$	U'u's7	P7	1384.4	1382.8	1.6
Σ^0	$1(3/2^+)$	U'd's7	P7-	1381.8	1383.7	-1.9
Σ^-	$1(3/2^+)$	D'd's7	N7-	1390.3	1387.2	3.1
Λ^0 (s_{01})	$0(1/2^-)$	U'd's7	P7-	1402.5	1406.0	-3.5
Λ^0 (D_{03})	$0(3/2^-)$	U'd's9	N9	1525.7	1519.5	6.2
<u>uss, dss</u>						
Ξ^0	$1/2(1/2^+)$	U'ss	NS1	1311.0	1314.9	-3.9
Ξ^-	$1/2(1/2^+)$	D'ss	NS1-	1315.6	1321.3	-5.7
Ξ^0	$1/2(3/2^+)$	U'ss4	N9+-	1533.7	1531.8	1.9
Ξ^-	$1/2(3/2^+)$	D'ss4	N10-	1530.3	1535.0	-4.7
Ξ^0	$1/2(3/2^-)$	U'ss9	N ₂ 1+-	1822.2	1823.0	-0.8
<u>udc, ddc, uuc</u>						
Λ_c^+	$0(1/2^+)$	U'd'c3	PS15	2290.0	2284.9	5.1
Σ_c^0	$1(1/2^+)$	D'd'c7	N ₂ 10	2452.5	2452.2	0.3
Σ_c^{++}	$1(1/2^+)$	U'u'c7	N ₂ 10++	2452.5	2452.8	-0.3
Σ_c^+	$1(1/2^-)$	U'd'c7	N ₂ 10+	2449.1	2453.6	-4.5
Λ_c^+	$0(1/2^-)$	U'd'c9	N ₂ 12+	2589.1	2593.9	-4.8
<u>usc, dsc</u>						
Ξ_c^+	$1/2(1/2^+)$	U'sc1	NS ₃ 8+	2467.3	2466.3	1.0
Ξ_c^0	$1/2(1/2^+)$	D'sc1	N S ₃ 8+-	2470.7	2471.8	-1.1
<u>sss</u>						
Ω^-	$0(3/2^+)$	Sss	NS6-	1665.7	1672.5	-6.8
<u>ssc</u>						
Ω_c^0	$0(1/2^+)$	Ssc	N ₂ S9	2705.2	2704.0	1.2
<u>bdb</u>						
Λ_b^0	$0(1/2^+)$	U'd'b1	N ₂ S ₉ 13	5631.5	5624.0	7.5

The full quark formula for baryons other than p and n involves hybrid quarks (u' and d'), vector quarks (s, c, and b), and pseudoscalar quark ($\pi_{1/2}$). The whole spectrum of baryons (other than p and n) follows the single $\pi_{1/2}$ series with 0, 1, 3, 4, 7, and $3n$. $\pi_{1/2}$ is

closely related to u and d, so the lowest energy state baryons (Λ and Σ) that contain low mass quark and high number of u or d have high number of $\pi_{1/2}$. On the contrary, the lowest energy state baryons (Ω , Ω_c , and Λ_b) that contain high mass quarks and no or low number of u and d have low number of $\pi_{1/2}$ or no $\pi_{1/2}$. $\pi_{1/2}$'s are added to the lowest energy state baryons to form the high-energy state baryons.

The basic fermion formula includes P, N, S, and $\pi_{1/2}$. If the dominant decay mode includes p, the basic fermion formula includes P. If the dominant decay mode includes n, the basic fermion formula includes N. If the decay mode does not include either n or p directly, the baryon with the dipole moment similar to p or n has the basic fermion formula with P or N, respectively. If the dipole moment is not known, the designation of P or N for the higher energy state baryon follows the designation of P or N for the corresponding lower energy state baryon. Only N is used in the multiple nucleons such as N_2 (two N's).

The result of calculated masses for light unflavored mesons is listed in Table 8. Light unflavored mesons have zero strange, charm, and bottom numbers.

Table 8. Light unflavored mesons

Meson	I (J ^{PC})	Full quark formula	Basic fermion formula	Calculated mass.	Observed mass	Difference
<u>J = 0, only u, d, or lepton in decay mode</u>						
π^0	1 (0 ⁺)	2	2	135.01	134.98	0.04
π^\pm	1 (0 ⁻)	2	2±	139.61	139.57	0.04
η	0 (0 ⁺)	8	8+-	548.0	547.3	0.7
η'	0 (0 ⁺)	14	14+-	958.1	957.8	0.3
η	0 (0 ⁺)	u'u'u'd'd'd'2	S ₃ 5+-	1292.6	1297.0	-4.4
f_0	0 (0 ⁺⁺)	u'u'u'd'd'd'6	S ₄ 4	1514.0	1500.0	14.0
<u>J > 0, only u, d, or lepton in decay modes</u>						
ρ	1 (1 ⁻)	ud2	S ₂ 2	770.2	769.3	0.9
ω	0 (1 ⁻)	ud2	S ₂ 2+-	785.4	788.6	-3.2
h_1	0 (1 ⁺)	ud8	S ₂ 8	1176.2	1170.0	6.2
ω	0 (1 ⁻)	Uudd2	S ₃ 7+-	1415.6	1419.0	-3.4
ω	0 (1 ⁻)	Uudd6	S ₄ 6	1650.0	1649.0	1.0
ω_3	0 (3 ⁻)	Uudd6	S ₄ 6	1662.0	1667.0	-5.0
<u>J = 0, u and d in major decay modes, s in minor decay modes</u>						
f_0	0 (0 ⁺⁺)	u'd's'4	14	980.4	980.0	0.4
a_0	1 (0 ⁺⁺)	u'd's'4	14	985.4	984.8	0.6
<u>J > 0, u and d in major decay modes, s in minor decay mode</u>						
a_1	1 (1 ⁺⁺)	Uds	S ₁₃	1232.7	1230.0	2.7
b_1	1 (1 ⁺)	Uds	S ₁₃	1232.7	1239.5	-6.8
f_2	0 (2 ⁺⁺)	uds1	S ₂ 9	1278.4	1275.4	3.0
f_1	0 (1 ⁺⁺)	uds1	S ₂ 9+-	1278.4	1281.9	-3.5
a_2	1 (2 ⁺⁺)	uds1	S ₁₄	1316.2	1318.1	-1.9
f_1	0 (1 ⁺⁺)	uds4	S ₃ 7	1429.7	1426.3	3.4
ρ	1 (1 ⁻)	uds4	S ₂ 12	1475.5	1465.0	10.5
π_2	1 (2 ⁺)	uds7	S ₂ 15	1685.5	1670.0	15.5
ρ_3	1 (3 ⁻)	uds7	S ₂ 15	1693.5	1691.0	2.5
ρ	1 (1 ⁻)	uds7	S ₂ 15+-	1698.6	1700.0	-1.4
f_4	0 (4 ⁺⁺)	uds12	S ₄ 7	2038.5	2034.0	4.5
<u>s in major decay modes</u>						
Φ	0 (1 ⁻)	ss-1	S ₃ +-	1017.6	1019.4	-1.8
f_2	0 (2 ⁺⁺)	ss7	S ₄ 4+-	1532.0	1525.0	7.0
Φ	0 (1 ⁻)	ss9	S ₄ 6+-	1672.1	1680.0	-7.9
Φ_3	0 (3 ⁻)	ss12	S ₆	1852.7	1854.0	-1.3
f_2	0 (2 ⁺⁺)	ss15	S ₆ 2	2000.7	2011.0	-10.3
f_2	0 (2 ⁺⁺)	ss18	N S ₃ 6	2299.3	2297.0	2.3
f_2	0 (2 ⁺⁺)	ss18	N S ₄ 2+-	2331.5	2339.0	-7.5

The full quark formulas for light unflavored mesons are different for different decay modes. There are three different types of the full quark formula for light unflavored mesons. Firstly, when the decay mode is all leptons or all mesons with u and d quarks, the full quark formula consists of $\pi_{1/2}$, u' , d' , u , and d quarks. Secondly, when u , d , and leptons are in the major decay modes, and s is in the minor decay modes, the full quark formula consists of $\pi_{1/2}$, u' , d' , s' , u , d , and s quarks. The most common full quark formula for such mesons is uds , which is essentially $\frac{1}{2}(u \bar{u} d \bar{d} s \bar{s})$. Finally, when s quarks are in the major or all decay mode, the full quark formula consists of $\pi_{1/2}$'s and s quarks. When $J = 0$, the full quark formula includes $\pi_{1/2}$'s and hybrid quarks (u' , d' , and s'). When $J > 0$, the full quark formula includes $\pi_{1/2}$'s and vector quarks (u , d , and s). Since there are double presence of u and d quarks for the full quark formula with u and d quark, it follows the double $\pi_{1/2}$ series: 0, 2, 6, 8, 14, and $6n$. The full quark formula with odd presence of u , d , and s follows the single $\pi_{1/2}$ series: 0, ± 1 , ± 3 , ± 4 , ± 7 , and $\pm 3n$.

The basic fermion formula includes $\pi_{1/2}$'s, S , and N . $\pi_{1/2} - \pi_{1/2}$ hadronic bond exists in the full quark formula with u and d quarks, and does not exist in the full quark formula with s quark. $S - S$ bond exists in all formula. Light unflavored mesons decay into symmetrical low mass mesons, such as 2γ , $3\pi^0$, and $\pi^0 2\gamma$ from η , or asymmetrical high and low mass mesons, such as asymmetrical $\pi^+ \pi \eta$, $\rho^0 \gamma$, and $\pi^0 \pi^0 \eta$ from η' . To distinguish the asymmetrical decay modes from the symmetrical decay modes, one “counter $\pi_{1/2} - \pi_{1/2}$ hadronic bond” is introduced in η' [32]. The binding energy for the counter $\pi_{1/2} - \pi_{1/2}$ hadronic bond is 5.04 MeV, directly opposite to -5.04 MeV for the $\pi_{1/2} - \pi_{1/2}$ hadronic bond. All light unflavored mesons with asymmetrical decay modes include this counter $\pi_{1/2} - \pi_{1/2}$ hadronic bonds. For an example, the mass of η' (14+-) is calculated as follows.

$$\begin{aligned} M_{\eta'} &= 14 M_{\pi_{1/2}} + 2 M_{e.m.} + E_{e.m.} + 7E_{\pi_{1/2} - \pi_{1/2}} - E_{\pi_{1/2} - \pi_{1/2}} \\ &= 958.2 \text{ MeV} \end{aligned} \quad (30)$$

The observed mass is 957.8 ± 0.14 MeV.

The result of the mass calculation for the mesons consisting of u , d , or s with s , c , or b is listed in Table 9.

Table 9. Mesons with s, c, and b

Meson	J^{pc}	Full quark formula	Basic fermion formula	Calculated mass.	Observed mass	Difference
<u>Light strange mesons</u>						
K^\pm	0^-	7	$7\pm$	494.8	493.7	1.1
K^0	0^-	7	$7+-$	498.2	497.7	0.5
K^*	0^+	$d's'14$	$S_2 11+-$	1413.4	1412.0	1.4
K^*	1^-	us	$S8\pm$	895.6	891.6	4.0
K^*	1^-	ds	$S8$	899.0	896.1	2.9
K_1	1^+	$ds6$	$S_2 9$	1273.4	1273.0	0.4
K_1	1^+	$ds8$	$S_2 11$	1405.4	1402.0	3.4
K^*	1^-	$ds8$	$S_2 11+-$	1413.4	1414.0	-0.6
$K^{*\pm}$	2^+	$us8$	$N7\pm$	1434.3	1425.6	8.7
K^*	2^+	$ds8$	$N7+-$	1437.7	1432.4	5.3
K^*	1^-	$ddss$	$S_3 11+-$	1717.8	1717.0	0.8
K_2	2^-	$ddss$	$N12$	1779.9	1773.0	6.9
K_3^*	3^-	$ddss$	$N12$	1779.9	1776.0	3.9
K_2	2^-	$ds14$	$S_4 8+-$	1812.1	1816.0	-3.9
K_4^*	4^+	$ds18$	$S_5 7+-$	2046.5	2045.0	1.5
<u>Charmed mesons</u>						
D^0	0^-	$u'c1$	$S_6 +-$	1860.7	1864.5	-3.8
D^\pm	0^-	$d'c1$	$S_6 \pm$	1857.3	1869.3	-12.0
D^{*0}	1^-	$uc1$	$S_6 2+-$	2000.7	2006.7	-6.0
$D^{*\pm}$	1^-	$dc1$	$S_6 2\pm$	1997.4	2010.0	-12.6
D_1	1^+	$uc7$	$S_6 8+-$	2420.9	2422.2	-1.3
D_2^*	2^+	$uc7$	$N S_4 4$	2463.6	2458.9	4.7
$D_2^{*\pm}$	2^+	$dc7$	$N S_4 4\pm$	2468.2	2459.0	9.2
<u>Charmed strange mesons</u>						
D_s	0^-	$s'c1$	$S_5 6$	1968.5	1968.6	0.1
D_{s1}	1^+	$sc4$	$NS18$	2535.4	2535.4	0.0
<u>Bottom mesons</u>						
B^\pm	0^-	$u'b$	$N_4 S20\pm$	5283.1	5279.0	4.1
B^0	0^-	$d'b$	$N_4 S20$	5278.5	5279.4	-0.9
B^*	1^-	db	N_6	5320.8	5325.0	-4.2
Bs	0^-	$s'b$	$N_5 S_3$	5373.5	5369.6	3.9

The full quark formula for these mesons contains $\pi_{1/2}$'s, u' , d' , s' , u , d , s , c , and b . The full quark formula for the mesons with $J = 0$ contains $\pi_{1/2}$, hybrid quarks (u' , d' , and s'), c , and b quarks. The full quark formula with $J > 0$ contains $\pi_{1/2}$'s and vector quarks (u , d , s , c , and b). Strange mesons have double presence of d and s , so it follows the double

$\pi_{1/2}$ series. All other mesons have single presence of u, d, or s, so they follow the single $\pi_{1/2}$ series. The basic fermion formula consists of $\pi_{1/2}$'s, S, and N. There is no $\pi_{1/2} - \pi_{1/2}$ bond. There are S – S and N – N bonds. For example, the mass of B_s ($N_5 S_3$) with the observed mass as 5369.6 ± 2 MeV is calculated as follows.

$$\begin{aligned} M &= 5M_N + 3M_S + (10+2)M_{S-S} \\ &= 5373.5 \text{ MeV} \end{aligned} \quad (31)$$

There are 10 S – S bonds for N_5 (two S – S bonds for each N) and 2 S – S bonds for S_3 .

The result of mass calculation for $c \bar{c}$ and $b \bar{b}$ mesons is listed in Table 10.

Table 10. $c \bar{c}$ and $b \bar{b}$ mesons

Meson	J^{PC}	Full quark formula	Basic fermion formula	Calculated mass.	Observed mass	Difference
<u>$C \bar{c}$ mesons</u>						
$\eta_c(1s)$	0^+	cc-6	$N S_3 15$	2982.3	2979.8	2.5
J/ψ	1^-	cc-3	$N_2 S_4$	3096.7	3096.9	-0.2
$\chi_c(1p)$	0^{++}	cc2	$N_2 S_2 14$	3415.5	3415.0	0.5
$\chi_c(1p)$	1^{++}	cc3	$N_2 S_4 6$	3516.8	3510.5	6.5
$\chi_{c2}(1p)$	2^{++}	cc4	$N_2 S_2 16$	3555.5	3556.2	-0.7
U_{2s}	1^-	cc6	$N_3 S 10$	3691.4	3686.0	5.4
ψ	1^-	cc7	$N_3 S 11$	3761.4	3769.9	-8.5
ψ	1^-	cc12	$N_4 7$	4037.4	4040.0	-2.6
ψ	1^-	cc14	$N_4 S 4$	4158.1	4159.0	-0.9
ψ	1^-	cc18	$N_4 S_2 3$	4418.8	4415.0	3.8
<u>$B \bar{b}$ mesons</u>						
$\Upsilon(1s)$	1^-	bb-12	$N_7 S_6 18$	9452.7	9460.3	-7.6
$\chi_b(1p)$	0^{++}	bb-4	$N_{10} S_3$	9860.3	9859.9	0.4
$\chi_{b1}(1p)$	1^{++}	bb-3	$N_{10} S 10$	9899.0	9892.7	6.3
$\chi_{b2}(1p)$	2^{++}	bb-3	$N_{10} 15$	9918.4	9912.6	5.8
$\Upsilon(2s)$	1^-	bb-1	$N_{10} S_2 7$	10019.7	10023.3	-3.6
$\chi_{b0}(1p)$	0^{++}	bb2	$N_{10} S_2 10$	10229.8	10232.1	-2.3
$\chi_{b1}(2p)$	1^{++}	bb2	$N_{10} S_4 1$	10261.1	10255.2	5.9
$\chi_{b2}(2p)$	2^{++}	bb2	$N_{10} S_4 1$	10261.1	10268.5	-7.4
$\Upsilon(3s)$	1^-	bb3	$N_{10} S_3 7$	10350.5	10355.3	-4.8
$\Upsilon(4s)$	1^-	bb7	$N_{11} S 7$	10575.7	10580.0	-4.3
Υ	1^-	bb12	$N_{12} 3$	10851.6	10865.0	-13.4
Υ	1^-	bb14	$N_{11} S_3 4$	11027.2	11019.0	8.2

The full quark formula contains c or b. Since it contains no u, d, or s related to $\pi_{1/2}$, it follows a mixed $\pi_{1/2}$ series from both the single $\pi_{1/2}$ series and the double $\pi_{1/2}$ series. Since c

and b are high mass quarks unlike the low mass u and d quarks that relate to $\pi_{1/2}$, the $\pi_{1/2}$ series actually starts from a negative $\pi_{1/2}$. The basic fermion formula contains $\pi_{1/2}$'s, S , and N . The only hadronic bond is $N - N$. An example is J/ψ ($N_2 S_4$) whose mass (3096.9 ± 0.04 MeV) is calculated as follows.

$$\begin{aligned} M &= 2 M_N + 4 M_S + 4 M_{S-S} \\ &= 3096.7 \text{ MeV} \end{aligned} \quad (32)$$

11. Conclusion

The cosmic evolutionary theory consists of three models: the object-vacuum model for the multiverse, the milky universe model for the observable expanding universe, and the periodic table of elementary particles for baryonic matter.

In the object-vacuum model, objects and vacuums evolve in different stages. The evolutionary sequence for the evolution of objects is string, membrane, particle, and then particle-wave. For vacuums, it is object vacuum, single vacuum, inclusive vacuum, and then exclusive vacuum. Object vacuum takes turn to coexist equally with object at the same location. Single vacuum exists with an object at the same location or different locations in one object to one vacuum relation. Inclusive vacuum exists at the same location with multiple objects. Exclusive vacuum excludes object at the same location.

Different universes in the multiverse are in different stages of evolution. Our observable expanding universe in one of the universes in the multiverse. The evolution of the expanding universe involves four stages: the pre-universe, the pre-expanding universe, the mixed pre-expanding universe, and the expanding universe.

The universe starts with the pre-universe where object and vacuum take turn to exist equally at the same location. It is an equilibrium state between vacuum and the pair of ten-dimensional superstring and anti-superstring with a non-zero vacuum energy. The vacuum fluctuation (Figs. 1, 2, 3, and 4) results in the pre-expanding universe with the chiral boundary positive charged 9-brane and the chiral boundary negative charged 9-antibrane separated by pregravity (the predecessor of gravity) and anti-pregravity. The collapse and the bounce of the pre-expanding universe result in the generation of the achiral mixed 9-particle with the multiple dimensional Kaluza-Klein structure, achiral pregravity, achiral anti-pregravity, and zero vacuum energy as shown in Fig. 5. The decrease in vacuum energy leads to the fractionalization of mixed 9-particles into mixed particles with lower energy and dimensions, resulting in the cosmic expansion in the form of the uneven supersymmetry transformation. The two modes, the big band and the big bang, of the cosmic expansion lead to two universes, the hidden universe and the observable universe, respectively as shown in Fig. 6. In the big bang mode, the superluminal inflation ruptures the connection among particles. The rupture brings about the big bang, cosmic radiation, elementary particles, dark matter, entropy, force fields, relativity, and quantum mechanics. The cosmic evolution related to objects and vacuums is shown in Fig. 7. Quantum mechanics explained by vacuums is shown in Fig. 15.

In the expanding universe, the hidden universe and the observable universe are incompatible until the mixed particles in the hidden universe are converted to mixed 3-particles compatible to the empty mixed 3-particles in the observable universe. The compatible universes lead to the emergence of dark energy that causes accelerated cosmic expansion in the observable universe as shown in Fig. 13. The increase in the fine structure constant relates to the emergence of this time dependent dark energy. The contraction of the hidden universe from the mixed 3-particle to the mixed 4-particle brings about the contraction in the observable universe. Eventually, both universes are back to the mixed pre-expanding universe to start another cycle. The cosmic evolution involves cyclic universe: the pre-universe, the pre-expanding universe, the mixed pre-expanding universe, the expanding universe, the compatible universes with dark energy, the contracting universe, and back to the mixed pre-expanding universe as Fig. 14.

For the observable universe, the model is the Milky Universe model (Fig. 12). In the Milky Universe model, baryonic matter with four-dimensional space-time is incompatible with dark matter with higher dimensional space-time (Fig. 8). Both of them are compatible with cosmic radiation. The incompatibility increases with the increasing size of the universe. Such incompatibility brings about the formation of inhomogeneous structure (anisotropies in the CMB) where the baryonic matter domains surrounded by the dark matter halos as oil droplets surrounded by water in emulsion. The five periods (Fig. 12) of baryonic structure development in the order of increasing incompatibility between baryonic matter and dark matter are the free baryonic matter, the baryonic droplet, the galaxy, the cluster, and the supercluster periods. The transition to the baryonic droplet generates density perturbation in the CMB. The transition from the baryonic droplet to galaxy is through the big eruption for the formations of the first-generation galaxies, including elliptical, normal spiral (Fig. 10), barred spiral (Fig. 11), irregular, and dwarf spheroidal galaxies. The transitions to cluster and supercluster are the mergers and interactions of galaxies for the formation of the second-generation galaxies, including modified giant ellipticals, cD, evolved S0, dwarf elliptical, BCD, and tidal dwarf galaxies. The universe now is in the early part of the supercluster period. The whole observable expanding universe behaves as one unit of emulsion with increasing incompatibility between dark matter and baryonic matter.

The model for baryonic matter is the periodic table of elementary particles. There is duality between the cosmic evolution and physical laws. Derived from the cosmic evolution, baryonic matter has the dimensional orbital that resembles to atomic orbital. The dimensional orbital constitutes the periodic table of elementary particles (Fig. 17 and Table 2) to account for all leptons, quarks, and gauge bosons. The calculated masses (Tables 1 and 3) of gauge bosons, leptons, and quarks derived from the periodic table are in good agreement with the observed values. For example, the calculated mass (176.5 GeV) of the top quark has an excellent agreement with the observed mass (174.3 ± 5.1 GeV).

A hadron can be represented by the full quark formula (Table 4) and the basic quark formula (Table 5). The full quark formula consists of all quarks, pseudoscalar quark in pion, and the hybrid quarks. The basic quark formula consists of the lowest mass quarks. The relation between these two formulas is expressed by Eq. (15). As a molecule is the composite of atoms with chemical bonds, a hadron is the composite of elementary particles with

"hadronic bonds" (Table 6) which are the overlappings of the auxiliary dimensional orbits. The calculated masses (Tables 7, 8, 9, and 10) of hadrons are in good agreement with the observed values. For examples, the calculated masses for neutron and pion are 939.54 and 135.01MeV in excellent agreement with the observed masses, 939.57 and 134.98 MeV, respectively. The overall standard deviation between the calculated masses and the observed masses for all hadrons (108 hadrons) is 5.1 MeV, comparing to ± 11.4 MeV, the average observed error for the masses of the hadrons.

The masses of gauge bosons, leptons, quarks, and hadrons can be calculated using only four known constants: the number of the extra spatial dimensions in the eleven dimensional membrane, the mass of electron, the mass of Z° , and α_e . The periodic table of elementary particles derived from the cosmic evolution provides the most comprehensive explanation and calculation for the masses of elementary particles and hadrons.

References

- * chung@wayne.edu
- [1] A. Valentini, quant-ph/0112151, quant-ph/0104067, quant-ph/0203049
- [2] L. Randall and R. Sundrum, Nucl. Phys. **B557** (1999) 79; Phys. Rev. Lett. **83** (1999) 3370 ; Phys. Rev. Lett. **83** (1999) 4690
- [3] P. Horava and E. Witten, Nucl. Phys. **B475** (1996) 94 [hep-th/9603142].
- [4] J. Khoury, B. A. Ovrut, P. J. Steinhardt, and N. Turok, hep-th/0103239; R. Kallosh, L. Kofman, and A. Linde, hep-th/0104073; S. Rasanen, hep-th/0111279.
- [5] G. Dvali, Q. Shafi, and S. Solganik, hep-th/0105203; C. P. Burgess, M. Majumdar, D. Nolte, F. Quevedo, G. Rajesh, and R. J. Zhang, hep-th/0105204.
- [6] A. Mazumdar, Phys.Lett. **B469** (1999) 55 [hep-ph/9902381]; A. Riotto, Phys. Rev. D **61** (2000) 123506; J. M. Cline, Phys. Rev. D **61** (2000) 02313; G. Dvali and S. H. H. Tye, Phys. Lett. **B450** (1999) 72; G. Shiu and S. H. H. Tye, hep-th/0106274; M. Bucher, hep-th/0107148; A. Nornov, hep-th/0109090; M.F. Parry, D. A. Steer, hep-th/0109207, D. Langlois, K. Maeda, D. Wards, gr-qc/0111013; J. Garriga, T. Tanaka, hep-th/0112028, S. Mukherji and M. Peloso, hep-th/0205180, P. Brax and D. A. Steer, hep-th/0207280, Y. S. Myung, hep-th/0208086
- [7] J. Khoury, B. A. Ovrut, N. Seiberg, P. J. Steinhardt, and N. Turok, hep-th/0108187; P. J. Steinhardt, and N. Turok, hep-th/0111098; P. J. Steinhardt, and N. Turok, astro-ph/0112537; J. Martin, P. Peter, N. Pinto-Neto, and D. Schwarz, hep-th/0112128; P. Steinhardt and N. Turok, astro-ph/0204479, R. Dave, R. R. Caldwell, P. J. Steinhardt, astro-ph/0206372
- [8] D. Chung, hep-ph/0003237, D. Chung, Speculations in Science and Technology 20 (1997) 259; Speculations in Science and Technology 21(1999) 277
- [9] A. Linde, Phys. Rev D**49** (1994) 748 [hep-ph/9307002], G. Felder, J. Garcia-Bellido, P. B. Greene, L. Kofman, A. Linde, I. Tkachev, Phys. Rev. Lett. **87** (2001) 011601 [hep-ph/0012142]; C. Herdeiro, S. Hirano, and R. Kallosh, hep-th/0111147.

- [10] D. Tytler, S. Burles, L. Lu, X-M, Fan, A. Wolfe, and B. Savage, *AJ*, **117** (1999) 63; F. C. van den Bosch, A. Burkert, and R. A. Swaters, *astro-ph/0105082*
- [11] A. H. Guth, *Phys. Rev. D* **23**, 347 (1981)
- [12] R. H. Bradenberger, *astro-ph/0208103*
- [13] M. Milgrom, *astro-ph/0207231*, *astro-ph/0112069*
- [14] F. Combes, *astro-ph/0206126*
- [15] R. Barkana and A. Loeb, *astro-ph/0209515*
- [16] B. M. Poggianti, *astro-ph/0210233*, S. F. Helsdon and T. J. Ponman, *astro-ph/0212047*
- [17] S. Leon, J. Braine, P. Duc, V. Charmandaris, and E. Brinks, *astro-ph/0208494*, *astro-ph/0210014*
- [18] M. Bonamente, M. Joy, and R. Liu, *astro-ph/0211439*
- [19] J. Einasto, G. Hutsi, M. Einasto, E. Saar, D. L. Tucher, V. Muller, P. Heinamaki, and S. S. Allam, *astro-ph/0212312*
- [20] M. J. West, *astro-ph/9709289*
- [21] N. Balcall, J.P. Ostriker, S. Perlmutter, and P.J. Steinhardt, *Science* **284**, 1481-1488, (1999); C. Armendariz-Picon, V. Mukhanov, and P.J. Steinhardt, *Phys.Rev.Lett.* **85**, 4438 (2000); K. Maeda, *astro-ph/0012313*; V. Sahni, *astro-ph/0202076*; D. Huterer, *astro-ph/0202256*.
- [22] J. K. Webb, M. T. Murphy, V. A. Flambaum, J. D. Dzuba, J. D. Barrow, C. W. Churchill, J. X. Prochaska, and A. M. Wolfe, *Phys. Rev. Lett.* **87**, 09130 (2001).
- [23] J. L. Martinez-Ledesma and S. Mendoza, *astro-ph/0210444*
- [24] P. Langacher, M. Luo, and A. Mann, *Rev. Mod. Phys.* **64** (1992) 87.
- [25] A. O. Barut and D. Chung, *Lett. Nuovo Cimento* **38** (1983) 225
- [26] SLD Collaboration, *Phys. Rev. D* **50** (1994) 5580
- [27] A.O. Barut, *Phys. Rev. Lett.* **42** (1979) 1251
- [28] L. Hall, R. Jaffe, J. Rosen1985, *Phys. Rep.* **125** (1985) 105
- [29] C.P. Singh, *Phys. Rev. D* **24** (1981) 2481; D. B. Lichtenberg *Phys. Rev. D* **40** (1989) 3675
- [30] D.E. Groom et al, *The European Physical Journal* **C15** (2000) 1
- [31] G.E. Brown, M. Rho, V. Vento, *Phys Lett* **97B** (1980); G.E. Brown, *Nucl. Phys.* **A374** (1982) 630
- [32] M.H. MacGregor, *Phys. Rev. D* **9** (1974) 1259; *Phys. Rev. D* **10** (1974) 850; *The Nature of the Elementary Particles* (Springer-Verlag, New York, 1978)